Disproportionation and electronic phase separation in parent manganite $LaMnO_3$

A. S. Moskvin
Ural State University, 620083 Ekaterinburg, Russia

(Received 22 September 2008; revised manuscript received 7 December 2008; published 4 March 2009)

Nominally pure undoped parent manganite $LaMnO_3$ exhibits a puzzling behavior inconsistent with a simple picture of an *A*-type antiferromagnetic insulator (A-AFI) with a cooperative Jahn-Teller ordering. We do assign its anomalous properties to charge transfer (CT) instabilities and competition between insulating A-AFI phase and metalliclike dynamically disproportionated phase formally separated by a first-order phase transition at $T_{disp}=T_{JT}\approx 750$ K. The unconventional high-temperature phase is addressed to be a specific electron-hole (EH) Bose liquid (EHBL) rather than a simple "chemically" disproportionated $La(Mn^{2+}Mn^{4+})O_3$ phase. The phase does nucleate as a result of the CT instability and evolves from the self-trapped CT excitons or specific EH dimers, which seem to be a precursor of both insulating and metalliclike ferromagnetic phases observed in manganites. We arrive at highly frustrated system of triplet $(e_g^2)^3A_{2g}$ bosons moving in a lattice formed by hole Mn^{4+} centers. Starting with different experimental data we have reproduced a typical temperature dependence of the volume fraction of high-temperature mixed-valence EHBL phase. We argue that a slight nonisovalent substitution, photoirradiation, external pressure, or magnetic field gives rise to an electronic phase separation with a nucleation or an overgrowth of EH droplets. Such a scenario provides a comprehensive explanation of numerous puzzling properties observed in parent and nonisovalently doped manganite $LaMnO_3$ including an intriguing manifestation of superconducting fluctuations.

DOI: 10.1103/PhysRevB.79.115102 PACS number(s): 71.30.+h, 75.47.Lx, 71.35.−y

I. INTRODUCTION

Perovskite manganites $RMnO_3$ (R=rare earth or yttrium) manifest many extraordinary physical properties. Undoped $TbMnO_3$ and $DyMnO_3$ reveal multiferroic behavior.[1] Under nonisovalent substitution all the orthorhombic manganites reveal an insulator-to-metal (IM) transition and colossal magnetoresistance (CMR) effect which are currently explained in terms of an electronic phase separation (EPS) triggered by a hole doping. Overview of the current state of the art with theoretical and experimental situation in doped CMR manganites $R_{1-x}Sr(Ca)_xMnO_3$ can be found in many review articles.[2–6]

However, even nominally pure undoped stoichiometric parent manganite $LaMnO_3$ does exhibit a puzzling behavior inconsistent with a simple picture of an *A*-type antiferromagnetic insulator (A-AFI) which it is usually assigned to.[2–6] First it concerns anomalous transport properties,[7–9] photoinduced (PI) absorption,[10] pressure-induced effects,[11] dielectric anomalies,[12] and the high field-induced IM transition.[13] Below, in the paper we demonstrate that the unconventional behavior of parent manganite $LaMnO_3$ can be explained to be a result of an electronic phase separation inherent even for nominally pure stoichiometric manganite with a coexistence of conventional A-AFI phase and unconventional electron-hole (EH) Bose liquid (EHBL) which nucleation is a result of a charge transfer (CT) instability of A-AFI phase. In a sense, hereafter we report a comprehensive elaboration of a so-called "disproportionation" scenario in manganites which was addressed earlier by many authors; however, by now it was not properly developed.

The paper is organized as follows. In Sec. II we discuss an unconventional first-order phase transition in parent manganite $LaMnO_3$ and argue that it should be addressed to be a disproportionation rather than a Jahn-Teller (JT) phase transition. Then we show that the resonant x-ray scattering data can be used to reconstruct a "phase diagram" which shows a tentative temperature dependence of the volume fraction of two competing phases for parent $LaMnO_3$. The electron-lattice relaxation effects and the self-trapping of the CT excitons with nucleation of electron-hole droplets are considered in Sec. III. In Sec. IV we describe the details of the charge and spin structure of electron-hole dimers to be the main building blocks of the EHBL phase in a parent manganite. The effective Hamiltonian of the EHBL phase equivalent to a triplet boson double-exchange (DE) model is addressed in Sec. V. Numerous optical, magnetic, and other manifestations of the EH dimers and EH droplets in parent and low-hole-doped manganites are considered in Sec. VI. Short comments on the hole doping effects are made in Sec. VII. Short conclusions are presented in Sec. VIII.

II. EXPERIMENTAL SIGNATURES OF DISPROPORTIONATION AND ELECTRONIC PHASE SEPARATION IN PARENT MANGANITE $LaMnO_3$

A. Unconventional first-order phase transition in $LaMnO_3$

Measurements on single crystals of the high-temperature transport and magnetic properties,[7–9,14] resonant x-ray scattering,[15,16] and neutron-diffraction[17] studies of the $RMnO_3$ family point to a first-order *electronic* phase transition at $T=T_{JT}$ ($T_{JT}\approx 750$ K in $LaMnO_3$) from the low-temperature orbitally ordered (OO) antiferromagnetic insulating phase (O′ orthorhombic *Pbnm*), with a cooperative Jahn-Teller ordering of the occupied orbitals of the MnO_6 octahedra to a high-temperature charge and orbitally disordered phase (O orthorhombic or "pseudocubic" *Pbnm*). It is worth noting that the "first orderness" is rather unexpected point for the cooperative Jahn-Teller ordering as a common

viewpoint implies that it is to be a second-order "order-disorder-type" phase transition. According to the conventional model of the first-order phase transitions, there are two characteristic temperatures, $T_1^* < T_{JT}$ and $T_2^* > T_{JT}$ ("supercooling" and "superheating" spinodals, respectively), which determine the temperature range of the coexistence of both phases. Both temperatures are hardly defined for parent manganites. A change in slope of the temperature dependence of the thermoelectric power at $T_1^* \approx 600$ K in $LaMnO_3$ (Refs. 9 and 14) is considered to be due to nucleation of an orbitally disordered phase on heating or homogeneous nucleation of the low-T OO phase on cooling. The volume fraction of charge and orbitally disordered phase monotonically grows with increasing temperature in the interval $T_1^* < T < T_{JT}$ but increases discontinuously on heating across T_{JT}. The low-T OO phase looses stability only at $T_2^* > T_{JT}$. Weak diffuse x-ray scattering consistent with orbital fluctuations was observed in $LaMnO_3$ with the intensity falling gradually with increasing temperature and disappearing above $T_2^* \sim 1000$ K concomitant with the suppression of the octahedral tilt ordering and a structural transition to a rhombohedral phase.[16]

The x-ray diffraction data[18] for $LaMnO_3$ have revealed a coexistence of two orthorhombic *Pbnm* phases O′ and O in a wide temperature range both below and above T_{JT}. It means that a sizable volume fraction of large (~1000 Å) domains of low- (high-) temperature phase survives between T_{JT} and T_2^* (T_1^* and T_{JT}), respectively. However, it does not prevent the nanoscopic size droplets to survive outside this temperature range. Furthermore, the neutron-diffraction measurements ($T < 300$ K) for several samples of nominal composition $LaMnO_3$ after different heat treatments seemingly provoking the nucleation of a high-temperature phase[19] have revealed a coexistence of bare orthorhombic A-AFI phase with another orthorhombic and rhombohedral ferromagnetic phases with a considerably (~2%) smaller unit-cell volume and ordering temperatures T_C near T_N. Puzzlingly, this coexistence spreads out over all temperature range studied from room temperature up to 10 K. Similar effects have been observed in a complex (ac initial magnetic susceptibility, magnetization, magnetoresistance, and neutron-diffraction) study ($T < 300$ K) of slightly nonstoichiometric $LaMnO_{3+\delta}$ system.[20] Interestingly that all over the ferromagnetic phases the thermal factors of oxygen atoms present an excess $\Delta B \sim 0.3-0.5$ Å^2 as compared with antiferromagnetic A-AFI phase that points to a specific role of dynamic lattice effects.

Even in the absence of chemical doping, $LaMnO_3$ shows the ability to accommodate a so-called "oxidative nonstoichiometry," which also involves the partial oxidation of some Mn^{3+} to Mn^{4+} which smaller size leads to an increase in the tolerance factor, thus stabilizing the perovskite structure.[21] The manganite crystals grown by the floating zone method seem to preserve well-developed traces of the high-temperature phase. Interestingly, that the $LaMnO_3$ crystals do not tolerate repeated excursions to high temperatures, 800 K, before changing their properties. Such an anomalous memory effect with an overall loss of long-range orbital order in one sample of the $LaMnO_3$ after extended cycling above 1000 K and cooling back to room temperature was observed by Zimmermann *et al.*[16] It is worth mentioning that the characteristic temperatures T_1^*, T_{JT}, and T_2^* for the phase transition are believed to depend on the initial content of Mn^{4+} (Ref. 17): the sample used in Ref. 22 gave $T_{JT}=600$ K and $T_2^*=800$ K, suggesting the presence of a non-negligible amount of Mn^{4+} that reduces the temperatures of the phase transition. All these data evidence an existence of electronic phase separation inherent for parent stoichiometric $LaMnO_3$ with the phase volume fraction sensitive to sample stoichiometry, prehistory, and morphology.

B. Disproportionation rather than the JT nature of the phase transition in parent $LaMnO_3$

The electronic state in the high-temperature O orthorhombic phase of parent $LaMnO_3$ remains poorly understood. The transport measurements[9] [resistivity $\rho(T)$ and thermoelectric power $\alpha(T)$; see, also Refs. 7, 8, 23, and 24] were interpreted by the authors as a striking evidence of the $R(Mn^{2+}Mn^{4+})O_3$ disproportionation rather than a simple orbitally disordered $RMn^{3+}O_3$ character of the high-temperature phase. Let us shortly overview the argumentation by Zhou and Goodenough.[9] Thermoelectric power reveals an irreversible change from $\alpha(300\ \mathrm{K}) = -600\ \mu\mathrm{V/K}$ to about $550\ \mu\mathrm{V/K}$ on thermal cycling to 1100 K with a nearly zero value at $T > T_{JT}$. Small-polaron conduction by a single charge carrier would give a temperature-independent thermoelectric power dominated by the statistical term

$$\alpha = -(k/e)\ln[(1-c)/c], \tag{1}$$

where c is the fraction of Mn sites occupied by a charge carrier and the spin degree of freedom is lifted by the strong intra-atomic exchange. Near stoichiometry, two types of charge carriers may be present but with only one dominating at room temperature to give a large negative or large positive $\alpha(300\ \mathrm{K})$ for a small value of c. From Eq. (1) value of $\alpha(300\ \mathrm{K}) \approx \pm 600\ \mu\mathrm{V/K}$ in the virgin crystal reflects a small fraction ($c \approx 0.001$) of a imbalance between electron-like and holelike mobile/immobile charges. An abrupt drop in $\alpha(T)$ and $\rho(T)$ at T_{JT} to a nearly temperature-independent and a nearly zero value for $T > T_{JT}$ with a reversible behavior of both quantities agrees with a phase transition to a fully disproportionated $Mn^{2+}+Mn^{4+}$ or, more precisely, to an electron-hole liquid phase[25–27] with a two-particle transport and $c_{eff}=0.5$. However, the system retains a rather high value of resistivity, that is, the EH liquid phase manifests a "poor" metal behavior. Strictly speaking, the disproportionation phase transition at $T=T_{disp}=T_{JT}$ is governed first by a charge order rather than the orbital order parameter. In other words, the Jahn-Teller ordering at $T=T_{JT}$ only accompanies the charge ordering at $T=T_{disp}=T_{JT}$; hence a simplified Jahn-Teller picture does misinterpret a true sense of the phenomenon.

In contrast with the high-temperature measurements carried out in a vacuum of 10^{-3} torr,[9] the transport measurements performed in air[28] evidenced another evolution of $\alpha(T)$ (see Fig. 1). On heating the thermoelectric power starts from large but *positive* values and on cooling from $T > T_{JT}\alpha(T)$ does not return to its original value because the sample, according to authors,[28] becomes slightly (~1%) oxi-

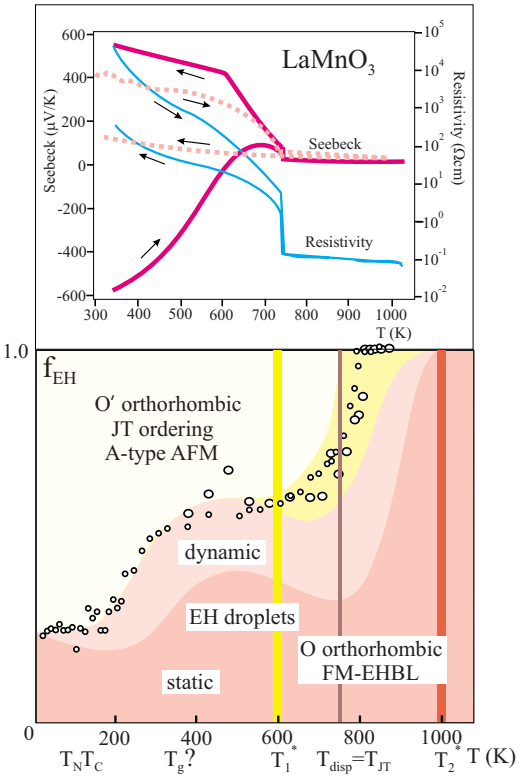

FIG. 1. (Color online) Top panel: temperature dependence of thermoelectric power and resistivity in parent manganite $LaMnO_3$ (reproduced from Refs. 9 and 28). Bottom panel: schematic T-f_{EH} phase diagram of a parent perovskite manganite, f_{EH} being the volume fraction of mixed-valence phase. Small and large circles show up experimental data from Refs. 15 and 16 transformed into a resultant volume fraction of a non-OO phase supposed to be a system of static and dynamic EH droplets. Different filling (from top to bottom) points to an A-AFI phase, orbital fluctuation phase near T_{JT}, and dynamic and static EH droplet phase. Note a difference in T_{JT} values in Refs. 15 and 16 and Ref. 9.

dized. A simple comparison of the two data sets[9,28] points to an unconventional behavior of parent manganite on crossing the "supercooling spinodal" temperature T_1^*. The system can memorize a high-temperature phase up to temperatures below 300 K. The role of a slight oxidation seemingly reduces to be an additional regulative factor governing the A-AFI/EHBL phase volume fraction.

Strong and irreversible temperature dependence of $\alpha(T)$ and $\rho(T)$ at $T<T_1^*$ agrees with a scenario of a well-developed electronic phase separation with a puzzling electron-hole symmetry and a strong sensitivity of transport properties both to sample morphology and quality. The magnitude of the resistivity and character of irreversibility agrees with a *poor metal* like conductivity of high-temperature phase and points to a considerable volume fraction of this phase to survive up to room temperature. Resistivity of different samples of the nominally same composition can differ by orders of magnitude. Interestingly that these data point to a possibility of colossal, up to 6 orders of magnitude, variations in resistivity in parent $LaMnO_3$ at a constant temperature well below T_{JT} only due to the variation in its A-AFI/EHBL volume fraction composition which can be realized by the temperature change, pressure, isotopic substitution, application of external magnetic/electric field, and photoirradiation. This behavior can hardly be directly related with the colossal magnetoresistivity observed for the hole doped manganites; however, this phase can be an important participant of electronic transformations in manganites.

Below $T=T_1^*$ ($T_1^*\approx 600$ K in $LaMnO_3$) or the temperature of the homogeneous nucleation of the low-T OO phase, the high-temperature mixed-valence EH phase loses stability, however, it survives due to various charge inhomogeneities forming EH droplets pinned by statically fluctuating electric fields.

C. Temperature dependence of the EHBL volume fraction

By now we have no information about how both phases share the volume fraction on cooling from high temperatures. Clearly, such an information depends strongly on the techniques used. For instance, both long-lived static domains and short-lived dynamic fluctuations of either phase contribute to optical response, while only the large static domains are seen in conventional x-ray or neutron scattering measurements. Fortunately, the resonant x-ray scattering data[15,16] can be used to reconstruct the tentative T-f_{EH} phase diagram of a manganite with f_{EH} being a volume fraction of EH droplets. Indeed, the intensity of this scattering depends on the size of the splitting Δ of the Mn $4p$ levels, induced by the orbital ordering of Mn $3de_g$ states, hence is nonzero only for orbitally ordered Mn^{3+} ions in distorted MnO_6 octahedra. The first-order nature of the cooperative JT phase transition in $LaMnO_3$ (Ref. 9) implies that the local orbital order parameter such as Δ in Ref. 15 remains nearly constant below the transition temperature;[29] hence the temperature behavior of resonant x-ray scattering intensity has to reflect the temperature change in the net (static+dynamic) OO phase volume fraction rather than $\Delta(T)$ effect. This suggestion agrees with the neutron-diffraction studies by Rodríguez-Carvajal *et al.*,[17] evidencing no visible effect of the antiferromagnetic spin ordering at $T=T_N\approx 140$ K on the OO parameter, while the x-ray scattering intensity dramatically (up to 40%) falls upon heating above T_N.[15] Overall, the temperature dependence of the resonant x-ray scattering intensity in $LaMnO_3$ shows up an unusual behavior with an arrest or even clear hole between 300 and 500 K, a sharp downfall above $T=T_1^*\approx 600$ K, and vanishing right after $T=T_{JT}\approx 750$ K. Thus, the x-ray data[15,16] can be used to find the temperature behavior of the resultant static and dynamic EH droplet volume fraction in the sample.

In Fig. 1 we have reproduced experimental data from Refs. 15 and 16 renormalized and transformed into a relative volume fraction of a "non-OO" phase which is supposed to be an EH droplet phase. The renormalization implied the low-temperature 75% volume fraction of the OO phase. Different filling (from top to bottom) points to an A-AFI phase, orbital fluctuation phase near T_{JT}, and dynamic and static EH droplet phase. Despite the overall fall of the EH droplet volume fraction on cooling from T_{JT}, we expect some intervals of the re-entrant behavior due to a subtle competition of two phases. It is clear that any ordering does lower the free en-

ergy of the phase thus resulting in a rise of its volume fraction. Taking into account experimental data from Ref. 19 pointing to close temperatures of AFI and ferromagnetic insulator (FI) orderings in competing phases (T_N and T_C, respectively), we may assign a signature of a re-entrant behavior at 400–600 K to a glasslike transition within the EH liquid near $T=T_g\sim 400$ K. Surely, we are aware that the picture shown in Fig. 1 is not a real phase diagram; however, it is very instructive for a qualitative understanding of a complex phase competition in parent manganite.

Concluding the section, we should once more emphasize a dramatic charge instability of parent manganite $LaMnO_3$ with extreme sensitivity to different external factors, sample stoichiometry, and prehistory. In this connection, it is worth noting that highly stoichiometric $LaMnO_3$ samples measured by Subías *et al.*[30] did not show noticeable temperature dependence of the resonant intensity for the (3,0,0) reflection from 10 to 300 K, in contrast with the data by Murakami *et al.*[15] Further work at an even higher temperature range and for different samples seems to be necessary in order to distinctly reveal and examine the phase-separated state in a parent manganite.

III. ELECTRON-LATTICE RELAXATION AND NUCLEATION OF EH DROPLETS IN A PARENT MANGANITE

A. Electron-lattice relaxation and self-trapping of CT excitons

At first glance the disproportionation in manganese compounds is hardly possible since manganese atom does not manifest a valence-skipping phenomenon as, e.g., bismuth atom which can be found as Bi^{3+} or Bi^{5+}, but not Bi^{4+}, with a generic bismuth oxide $BaBiO_3$ to be a well-known example of a charge disproportionated system. Strictly speaking, sometimes manganese reveals a valence preference, e.g., while both Mn^{2+} and Mn^{4+} are observed in MgO:Mn and CaO:Mn, the Mn^{3+} center is missing.[31] Furthermore, the d^4 configuration of Mn^{3+} ion is argued[32] to be a missing oxidation state due to the large exchange-correlation energy gain that stabilizes the d^5 electronic configuration thus resulting in the charge disproportionation or dynamical charge fluctuation $d^4+d^4\rightarrow d^3+d^5$.

The reason for valence skipping or valence preference observed for many elements still remains a mystery. Recently, Harrison[33] argued that most likely traditional lattice relaxation effects, rather than any intra-atomic mechanisms (specific behavior of ionization energies, stability of closed shells, and strong screening of the high-charged states), are a driving force for disproportionation with formation of so-called "negative-*U*" centers.

Anyhow the disproportionation in an insulator signals a well-developed CT instability. What is a microscopic origin of the CT instability in parent manganites? The disproportionation reaction can be considered to be a final stage of a self-trapping of the *d-d* CT excitons (Mott-Hubbard excitons) that determine the main low-energy CT band peaked near 2 eV in $LaMnO_3$.[34] Indeed, these two-center excitations due to a charge transfer between two MnO_6 octahedra may be considered as quanta of the disproportionation reaction,

$$MnO_6^{9-}+MnO_6^{9-}\rightarrow MnO_6^{8-}+MnO_6^{10-}, \quad (2)$$

with the creation of electron MnO_6^{10-} and hole MnO_4^{8-} centers. Within a simplest model[26] the former corresponds to a nominal $3d^5$ (Mn^{2+}) configuration, while the latter does to the $3d^3$ (Mn^{4+}) one.

The minimal energy cost of the optically excited disproportionation or electron-hole formation in insulating manganites is 2.0–2.5 eV.[34] However, the question arises: what is the energy cost for the thermal excitation of such a local disproportionation or effective correlation energy *U*? The answer implies first of all the knowledge of relaxation energy or the energy gain due to the lattice polarization by the localized charges. The full polarization energy *R* includes the cumulative effect of electronic and *ionic* terms related with the displacement of electron shells and ionic cores, respectively.[35] The former term $R_{\rm opt}$ is due to the *nonretarded* effect of the electronic polarization by the momentarily localized electron-hole pair given the ionic cores fixed at their perfect crystal positions. Such a situation is typical for lattice response accompanying the Franck-Condon transitions (optical excitation and photoionization). On the other hand, all the long-lived excitations, i.e., all the intrinsic thermally activated states and the extrinsic particles produced as a result of doping, injection, or optical pumping, should be regarded as stationary states of a system with a deformed lattice structure.

The lattice relaxation energies, $-\Delta R_{\rm th}$, associated with the hole/electron localization in 3*d* oxides are particularly large. For instance, in $LaMnO_3$ the optical (nonrelaxed) energies of the creation of the hole on Mn and O sites are 2.6 and 4.9 eV, respectively, while $-\Delta R_{\rm th}^{\rm Mn}=0.7-0.8$ and $-\Delta R_{\rm th}^{\rm O}=2.4$ eV.[36] In other words, the electronic hole is marginally more stable at the Mn site than at the O site in the $LaMnO_3$ lattice; however, both possibilities should be treated seriously.

Shell-model estimations[36] yield for the energy of the optically excited disproportionation (2) or electron-hole formation in parent manganite $LaMnO_3$: $E_{\rm opt}\approx 3.7$ eV, while the respective thermal relaxation energy is estimated as $-\Delta R_{\rm th}\approx 1.0$ eV. Despite the estimations imply the noninteracting electron and hole centers these are believed to provide a sound background for any reasonable models of self-trapped *d-d* CT excitons. Thorough calculation of the localization energy for electron-hole dimers remains a challenging task for future studies. It is worth noting that despite their very large several eV magnitudes, the relaxation effects are not incorporated into current theoretical models of manganites.

Figure 2 illustrates two possible ways the electron-lattice polarization governs the CT exciton evolution. Shown are the adiabatic potentials (APs) for the two-center ground-state (GS) M^0-M^0 configuration and excited $M^{\pm}$-$M^{\mp}$ CT or disproportionated configuration. The *Q* coordinate is related with a lattice degree of freedom. For lower branch of AP in the system we have either a single minimum point for the GS configuration [Fig. 2(a)] or a two-well structure with an additional local minimum point [Fig. 2(b)] associated with the self-trapped CT exciton. This "bistability" effect is of primary importance for our analysis. Indeed, these two minima

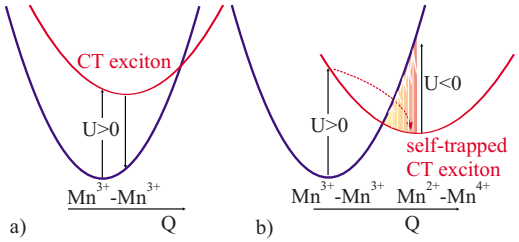

FIG. 2. (Color online) Simple illustration of the electron-lattice polarization effects for CT excitons (see text for details).

are related with two (meta)stable charge states with and without CT, respectively, which form two candidates to struggle for a ground state. It is worth noting that the self-trapped CT exciton may be described as a configuration with negative disproportionation energy U. Thus one concludes that all the systems such as manganites may be divided into two classes: *CT stable systems* with the only lower AP branch minimum for a certain charge configuration, and bistable, or *CT unstable systems* with two lower AP branch minima for two local charge configurations, one of which is associated with the self-trapped CT excitons resulting from self-consistent charge transfer and electron-lattice relaxation. Such excitons are often related with the appearance of the negative-U effect. It means that the three types of MnO_6 centers $MnO_4^{8,9,10-}$ should be considered in manganites on equal footing.[26,27]

Above we have presented a generalized disproportionation scenario for parent manganites in which an unconventional phase state with a $2Mn^{3+} \rightarrow Mn^{2+} + Mn^{4+}$ disproportionation nominally within manganese subsystem evolves from EH dimers or self-trapped d-d CT excitons. However, such a scenario in parent manganites would compete with another "asymmetric" disproportionation scenario,

$$Mn^{3+} + O^{2-} \rightarrow Mn^{2+} + O^{1-}, \tag{3}$$

which evolves from a self-trapping of low-energy p-d CT excitons. Indeed, we should make a remarkable observation, which to the best of our knowledge has not been previously reported for these materials, that is, the famous "manganite" 2 eV absorption band has a composite structure being a superposition of a rather broad and intensive CT d-d band and several narrow and relatively weak CT p-d bands.[34,37] A dual nature of the dielectric gap in nominally stoichiometric parent perovskite manganites $RMnO_3$, being formed by a superposition of forbidden or weak dipole allowed p-d CT transitions and intersite d-d CT transitions, means that these should rather be sorted neither into the CT insulator nor the Mott-Hubbard insulator in the Zaanen-Sawatzky-Allen[38] scheme. A detailed analysis of the CT p-d transitions in $LaMnO_3$ has been performed by the present author in Ref. 37. Among the first p-d candidates for a self-trapping we should point to the low-energy CT state $[(t_{2g}^3\,{}^4A_{2g}; e_g^2\,{}^3A_{2g}; {}^6A_{1g}); \underline{t}_{1g}]^{5,7}T_{1g}$ in MnO_6^{9-} octahedron which arises as a result of the O $2p$ electron transfer from the highest in energy nonbonding t_{1g} orbital to the e_g manganese orbital. Simplest view of this exciton implies the oxygen t_{1g} hole rotating around nominally Mn^{2+} ion with ferro-($^7T_{1g}$) or antiferro-($^5T_{1g}$) ordering. It has a number of unconventional properties. First, orbitally degenerated ground T_{1g} state implies a nonquenched orbital moment and strong magnetic anisotropy. May be more important to say that we deal with a Jahn-Teller center unstable with regard to local distortions. Second, we expect a high-spin $S=3$ ground state $^7T_{1g}$ because of usually ferromagnetic p-d exchange coupling. Oxygen holes can form the so-called O^- bound small polarons.[39]

Shell-model estimations[36] yield for the energy of optically excited asymmetric disproportionation (3) in parent manganite $LaMnO_3$: $E_{opt} \approx 4.75$ eV, while the respective thermal relaxation energy is estimated as $-\Delta R_{th} \approx 1.25$ eV. However, these qualitative estimations do not concern a number of important points such as p-d and p-p covalencies, and a partial delocalization of oxygen holes.

A sharp electron-hole asymmetry and a rather big $S=3$ ground-state spin value most likely exclude the self-trapped p-d CT excitons as candidates to form a high-temperature $T > T_{JT}$ phase of parent manganite. However, the "dangerous" closeness to the ground state makes them to be the potential participants of any perturbations taking place for parent manganites.

B. Nucleation of EH droplets in a parent manganite

The AP bistability in CT unstable insulators points to tempting perspectives of their evolution under either external impact. Metastable CT excitons in the CT unstable M^0 phase or EH dimers present candidate "relaxed excited states" to struggle for stability with ground state and the natural nucleation centers for electron-hole liquid phase. What way the CT unstable M^0 phase can be transformed into novel phase? It seems likely that such a phase transition could be realized due to a mechanism familiar to semiconductors with filled bands such as Ge and Si where given certain conditions one observes a formation of metallic EH liquid as a result of the exciton decay.[40] However, the system of strongly correlated electron M^- and hole M^+ centers appears to be equivalent to an electron-hole Bose liquid in contrast with the electron-hole Fermi liquid in conventional semiconductors. The Mott-Wannier excitons in the latter wide-band systems dissociate easily producing two-component electron-hole gas or plasma,[40] while small CT excitons both free and self-trapped are likely to be stable with regard to the EH dissociation. At the same time, the two-center CT excitons have a very large fluctuating electrical dipole moment $|d| \sim 2eR_{MM}$ and can be involved into attractive electrostatic dipole-dipole interaction. Namely, this is believed to be important incentive to the proliferation of excitons and its clusterization. The CT excitons are proved to attract each other and form molecules called biexcitons, and more complex clusters, or excitonic strings, where the individuality of the separate exciton is likely to be lost. Moreover, one may assume that like the semiconductors with indirect band gap structure, it is energetically favorable for the system to separate into a low density exciton phase coexisting with the microregions of a high density two-component phase composed of electron M^- and hole M^+ centers or EH droplets. Indeed, the excitons may be considered to be well defined entities only at small content,

whereas at large densities their coupling is screened and their overlap becomes so considerable that they loose individuality and we come to the system of electron M^- and hole M^+ centers, which form a metalliclike electron-hole Bose liquid with a main two-particle transport mechanism.[27] An increase in injected excitons in this case merely increases the size of the EH droplets, without changing the free exciton density.

An EH droplet seems to have no distinct boundary, most likely it looks like a core with more or less stable electron and hole centers surrounded by a cloud of metastable CT excitons. *Homogeneous nucleation* implies the spontaneous formation of EH droplets due to the thermodynamic fluctuations in exciton gas. Generally speaking, such a state with a nonzero volume fraction of EH droplets and the spontaneous breaking of translational symmetry can be stable in nominally pure insulating crystal. However, the level of intrinsic nonstoichiometry in $3d$ oxides is significant (one charged defect every 100–1000 molecular units is common). The charged defect produces random electric field, which can be very large (up to 10^8 V cm^{-1}) thus promoting the condensation of CT excitons and the *inhomogeneous nucleation* of EH droplets.

Deviation from the neutrality implies the existence of additional electron or hole centers that can be the natural centers for the inhomogeneous nucleation of the EH droplets. Such droplets are believed to provide a more effective screening of the electrostatic repulsion for additional electron/hole centers than the parent insulating phase. As a result, the electron/hole injection to the insulating M^0 phase due to a nonisovalent substitution as in $La_{1-x}Sr_xMnO_3$ or change in stoihiometry as in La_xMnO_3, $LaMnO_{3-\delta}$, or field effect is believed to shift the phase equilibrium from the insulating state to the unconventional electron-hole Bose liquid or in other words induce the insulator-to-EHBL phase transition. This process results in a relative increase in the energy of the parent phase and creates proper conditions for its competing with other phases capable to provide an effective screening of the charge inhomogeneity potential. The strongly degenerate system of electron and hole centers in EH droplet is one of the most preferable ones for this purpose. At the beginning (nucleation regime) an EH droplet nucleates as a nanoscopic cluster composed of several numbers of neighboring electron and hole centers pinned by disorder potential. It is clear that such a situation does not exclude the self-doping with the formation of a self-organized collective charge-inhomogeneous state in systems which are near the charge instability.

EH droplets can manifest itself remarkably in various properties of the $3d$ oxides even at small volume fraction or in a "pseudoimpurity regime." Insulators in this regime should be considered as phase inhomogeneous systems with, in general, thermoactivated mobility of the interphase boundaries. On the one hand, main features of this pseudoimpurity regime would be determined by the partial intrinsic contributions of the appropriate phase components with possible limitations imposed by the finite size effects. On the other hand, the real properties will be determined by the peculiar geometrical factors such as a volume fraction, the average size of droplets and its dispersion, the shape and possible texture of the droplets, and the geometrical relaxation rates. These factors are tightly coupled, especially near phase transitions for either phase (long-range antiferromagnetic ordering for the parent phase, the charge ordering, and other phase transformations for the EH droplets) accompanied by the variation in a relative volume fraction.

Numerous examples of the unconventional behavior of the $3d$ oxides in the pseudoimpurity regime could be easily explained with taking into account the interphase boundary effects (coercitivity, mobility threshold, non-Ohmic conductivity, oscillations, relaxation, etc.) and corresponding characteristic quantities. Under increasing doping the pseudoimpurity regime with a relatively small volume fraction of EH droplets (nanoscopic phase separation) can gradually transform into a macro(chemical) "phase-separation regime" with a sizable volume fraction of EH droplets and finally to another EH liquid phase.

IV. ELECTRON-HOLE DIMERS IN PARENT MANGANITE

A. EH dimers: Physical versus chemical view

Parent manganites are believed to be unconventional systems which are unstable with regard to a self-trapping of the low-energy charge transfer excitons which are precursors of nucleation of the EH Bose liquid. Hereafter we should emphasize once more that a view of the self-trapped CT exciton to be a Mn^{2+}-Mn^{4+} pair is typical for a *chemical* view of disproportionation and is strongly oversimplified. Actually we deal with an EH dimer to be a dynamically charge fluctuating system of coupled electron MnO_6^{10-} and hole MnO_4^{8-} centers having been glued in a lattice due to a strong electron-lattice polarization effects. In other words, we should proceed with a rather complex *physical* view of disproportionation phenomena which first implies a charge exchange reaction,

$$Mn^{2+} + Mn^{4+} \leftrightarrow Mn^{4+} + Mn^{2+}, \tag{4}$$

governed by a two-particle charge transfer integral,

$$t_B = \langle Mn^{2+}Mn^{4+}|\hat{H}_B|Mn^{4+}Mn^{2+}\rangle, \tag{5}$$

where $\hat{H}_B$ is an effective two-particle (bosonic) transfer Hamiltonian, and we assume a parallel orientation of all the spins. As a result of this quantum process the bare ionic states with site-centered charge order and the same bare energy E_0 transform into two EH-dimer states with an indefinite valence and bond-centered charge order,

$$|\pm\rangle = \frac{1}{\sqrt{2}}(|Mn^{2+}Mn^{4+}\rangle \pm |Mn^{4+}Mn^{2+}\rangle) \tag{6}$$

with the energies $E_\pm = E_0 \pm t_B$. In other words, the exchange reaction restores the bare charge symmetry. In both $|\pm\rangle$ states the site manganese valence is indefinite with quantum fluctuations between +2 and +4, however, with a mean value +3. Interestingly that, in contrast with the ionic states, the EH-dimer states $|\pm\rangle$ have both a distinct electron/hole and an inversion symmetry, even parity (s-type symmetry) for $|+\rangle$ and odd parity (p-type symmetry) for $|-\rangle$ states, respectively. Both states are coupled by a large electric-dipole matrix element,

$$\langle + |\hat{\mathbf{d}}| - \rangle = 2e\mathbf{R}_{\mathrm{MnMn}}, \tag{7}$$

where R_{MnMn} is a Mn-Mn separation. The two-particle transport Mn^{2+}-$Mn^{4+} \rightarrow Mn^{4+}$-$Mn^{2+}$ can be realized through two successive one-particle processes with the e_g-electron transfer as follows:

$$Mn^{2+} + Mn^{4+} \xrightarrow{e_g} Mn^{3+} + Mn^{3+} \xrightarrow{e_g} Mn^{4+} + Mn^{2+}.$$

Hence the two-particle transfer integral t_B can be evaluated as follows:

$$t_B = -t_{e_g}^2/U, \tag{8}$$

where t_{e_g} is one-particle transfer integral for e_g electron and U is a mean transfer energy. It means that the two-particle bosonic transfer integral can be directly coupled with the kinetic e_g contribution $J_{\mathrm{kin}}^{e_g}$ to Heisenberg exchange integral. Both t_B and $J_{\mathrm{kin}}^{e_g}$ are determined by the second-order one-particle transfer mechanism. It should be noted that negative sign of the two-particle CT integral t_B points to the energy stabilization of the s-type EH-dimer state $|+\rangle$.

Second, one should emphasize once more that the stabilization of EH dimers is provided by a strong electron-lattice effect with a striking intermediate oxygen atom polarization and displacement concomitant with charge exchange. In a sense, the EH dimer may be addressed to be a bosonic counterpart of the Zener Mn^{4+}-Mn^{3+} polaron.[41] It is no wonder that even in a generic disproportionated system $BaBiO_3$ instead of simple checkerboard charge ordering of Bi^{3+} and Bi^{5+} ions we arrive at charge-density wave (CDW) state with the alteration of expanded $Bi^{(4-\rho)+}O_6$ and compressed $Bi^{(4+\rho)+}O_6$ octahedra with $0 < \rho \ll 1$.[42] Enormously large values of oxygen thermal parameters in $BaBiO_3$ (Ref. 43) evidence a great importance of dynamical oxygen breathing modes providing some sort of a "disproportionation glue." Sharp rise of the oxygen thermal parameter in the high-temperature O phase of $LaMnO_3$ (Ref. 17) or in several "competing" phases found by Huang *et al.*[19] as compared with the bare AFI phase is believed to be a clear signature of the manganese disproportionation.

The formation of EH dimers seems to be a more complex process than it is assumed in simplified approaches such as Peierls-Hubbard model (see, e.g., Ref. 44) or Rice-Sneddon model.[45] As a rule, these focus on the breathing mode for the intermediate oxygen ion and neglect strong effects of the overall electron-lattice relaxation. The EH dimer can be viewed as a Jahn-Teller center (JT polaron) with the energy spectrum perturbed by strong electron-lattice effects. Thus we see that a simple chemical view of the disproportionation should be actually replaced by a more realistic physical view that implies a quantum and *dynamical* nature of the disproportionation reaction.

B. EH dimers: Spin structure

Let us apply to spin degrees of freedom which are of great importance for magnetic properties both of isolated EH dimer and of the EHBL phase that evolves from the EH dimers. The net spin of the EH dimer is $\mathbf{S}=\mathbf{S}_1+\mathbf{S}_2$, where $\mathbf{S}_1$ ($S_1=5/2$) and $\mathbf{S}_2$ ($S_1=3/2$) are spins of Mn^{2+} and Mn^{4+} ions, respectively. In nonrelativistic approximation the spin structure of the EH dimer will be determined by isotropic Heisenberg exchange coupling,

$$V_{\mathrm{ex}} = J(\hat{\mathbf{S}}_1 \cdot \hat{\mathbf{S}}_2), \tag{9}$$

with J being an exchange integral, and two-particle charge transfer characterized by a respective transfer integral which depends on spin states as follows:

$$\left\langle \frac{5}{2}\frac{3}{2}; SM \middle| \hat{H}_B \middle| \frac{3}{2}\frac{5}{2}; SM \right\rangle = \frac{1}{20} S(S+1) t_B, \tag{10}$$

where t_B is a spinless transfer integral. Making use of this relation we can introduce an effective spin-operator form for the boson transfer as follows:

$$\hat{H}_B^{\mathrm{eff}} = \frac{t_B}{20}[2(\hat{\mathbf{S}}_1 \cdot \hat{\mathbf{S}}_2) + S_1(S_1+1) + S_2(S_2+1)], \tag{11}$$

which can be a very instructive tool both for qualitative and quantitative analyses of boson transfer effects, in particular, the temperature effects. For instance, the expression points to a strong, almost twofold, suppression of effective transfer integral in paramagnetic phase as compared with its maximal value for a ferromagnetic ordering.

Both conventional Heisenberg exchange coupling and unconventional two-particle bosonic transfer or bosonic double exchange can be easily diagonalized in the net spin S representation so that for the energy we arrive at

$$E_S = \frac{J}{2}\left[S(S+1) - \frac{25}{2} \right] \pm \frac{1}{20} S(S+1) t_B, \tag{12}$$

where $\pm$ corresponds to two quantum superpositions $|\pm\rangle$ written in a spin representation as follows:

$$|SM\rangle_{\pm} = \frac{1}{\sqrt{2}}\left(\left| \frac{5}{2}\frac{3}{2}; SM \right\rangle \pm \left| \frac{3}{2}\frac{5}{2}; SM \right\rangle \right), \tag{13}$$

with s- and p-type symmetries, respectively. It is worth noting that the bosonic double-exchange contribution formally corresponds to ferromagnetic exchange coupling with $J_B = -\frac{1}{10}|t_B|$.

We see that the cumulative effect of the Heisenberg exchange and the bosonic double-exchange results in a stabilization of the $S=4$ high-spin (ferromagnetic) state of the EH dimer provided $|t_B| > 10J$ and the $S=1$ low-spin (ferrimagnetic) state otherwise. Spin states with intermediate S values, $S=2,3$, correspond to a classical noncollinear ordering.

To estimate both quantities t_B and J we can address the results of a comprehensive analysis of different exchange parameters in perovskites $R\mathrm{FeO}_3$, $R\mathrm{CrO}_3$, and $R\mathrm{Fe}_{1-x}\mathrm{Cr}_x\mathrm{O}_3$ with Fe^{3+} and Cr^{3+} ions[46] isoelectronic with Mn^{2+} and Mn^{4+}, respectively. For the superexchange geometry typical for $LaMnO_3$ (Ref. 21) with the Mn-O-Mn bond angle $\theta \approx 155°$ the authors have found $J = J(d^5 - d^3) = +7.2$ K while for $J(e_g e_g) \approx -t_B = 295.6$ K. In other words, for a net effective exchange integral we come to a rather large value: $J_{\mathrm{eff}} = J - 0.1|t_B| \approx 22.4$ K. Despite the antiferromagnetic sign of the Heisenberg superexchange integral these data unam-

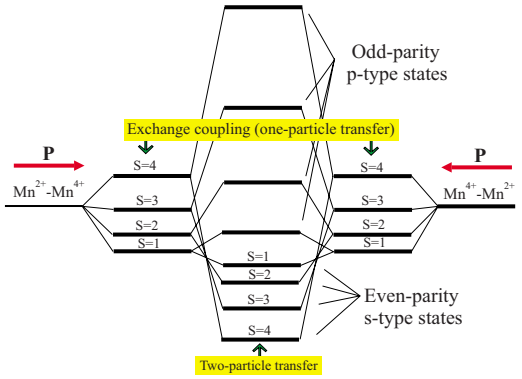

FIG. 3. (Color online) Spin structure of the self-trapped CT exciton or EH dimer with a step-by-step inclusion of one- and two-particle charge transfers. Arrows point to electric-dipole moment for bare site-centered dimer configurations.

biguously point to a dominant ferromagnetic contribution of the bosonic double-exchange mechanism.

It is worth noting that the authors[46] have predicted the sign change in the superexchange integral in the d^5-O^{2-}-d^3 system Fe^{3+}-O^{2-}-Cr^{3+} in perovskite lattice from the antiferromagnetic to ferromagnetic one on crossing the superexchange bonding angle $\theta \approx 162°$. Interestingly that the parameter $J(e_g e_g) \approx -t_B$ is shown to rapidly fall with the decrease in the bond angle θ in contrast with $J=J(d^5-d^3)$ which reveals a rapid rise with θ. For the bond angle $\theta=143°$ typical for the heavy rare-earth manganites $R\mathrm{MnO_3}$ (R=Dy, Ho, Y, Er) (Ref. 21) the relation between $t_B \approx -153.8$ K and $J=J(d^5-d^3) \approx 14.4$ K (Ref. 46) approaches to the critical one, $|t_B|=10J$, evidencing a destabilization of the ferromagnetic state for the EH dimers. In other words, the structural factor plays a significant role for stabilization of one or another spin state of the EH dimers. Spin structure of the EH dimer given antiferromagnetic sign of exchange integral $J>0$ and $|t_B|=20J$ is shown in Fig. 3. We see a dramatic competition of two opposite trends, governed by one- and two-particle transports.

EH dimers can manifest typical superparamagnetic behavior with large values of the effective spin magnetic moment up to $\mu_{\mathrm{eff}} \approx 9\mu_B$. Both bare Mn^{2+} and Mn^{4+} constituents of the EH dimer are s-type ions; i.e., these have an orbitally nondegenerated ground state that predetermines a rather small spin anisotropy.

Local magnetic fields on the manganese nuclei in both bond-centered $|SM\rangle_{\pm}$ states of the EH dimer are the same and determined as follows:

$$\mathbf{H}_n = \frac{1}{2}\left[\frac{S(S+1)+5}{2S(S+1)}A_2 + \frac{S(S+1)-5}{2S(S+1)}A_4\right]\langle \mathbf{S}\rangle, \quad (14)$$

where A_2 and A_4 are hyperfine constants for Mn^{2+} and Mn^{4+}, respectively, and we neglect the effects of transferred and supertransferred hyperfine interactions. Starting with typical for Mn^{2+} and Mn^{4+} values of $\frac{5}{2}A_2=600$ MHz and $\frac{3}{2}A_4=300$ MHz, respectively, we arrive at maximal values of ^{55}Mn nuclear magnetic resonance (NMR) frequencies for S=4, 3, 2, and 1 spin states of the EH dimer to be 450, 342.5, 237, and 135 MHz, respectively. The ^{55}Mn NMR frequencies for bare $Mn^{4+,3+,2+}$ ions in $LaMnO_3$ (Refs. 47–49) and theoretical predictions for the EH dimer in different spin states are shown in Fig. 4. Comparing these values with two bare frequencies we see that ^{55}Mn NMR can be a useful tool to study the EH dimers in a wide range from bond-centered to site-centered states. Experimental ^{55}Mn NMR signal for slightly nonstoichiometric $LaMnO_3$ (Ref. 50) is shown in Fig. 4 by filling (see Sec. VI for discussion).

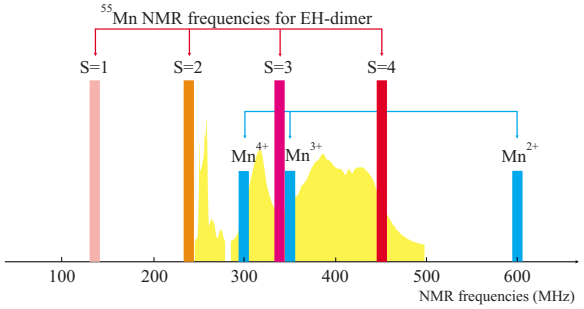

FIG. 4. (Color online) ^{55}Mn NMR frequencies for bare $Mn^{4+,3+,2+}$ ions in $LaMnO_3$ (Refs. 47–49) and theoretical predictions for the EH dimer in different spin states. Shown by filling is a ^{55}Mn NMR signal for slightly nonstoichiometric $LaMnO_3$ reproduced from Ref. 50.

Concluding the section we should point to unconventional magnetoelectric properties of the EH dimer. Indeed, the two-particle bosonic transport and respective kinetic contribution to stabilization of the ferromagnetic ordering can be suppressed by a relatively small electric field that makes the EH dimer to be a promising magnetoelectric cell especially for the heavy rare-earth manganites $R\mathrm{MnO_3}$ (R=Dy, Ho, Y, Er) with supposedly a ferroantiferroinstability. In addition, it is worth noting a strong anisotropy of the dimer's electric polarizability. In an external electric field the EH dimers tend to align along the field.

C. EH-dimer dynamics: Immobile and mobile dimers

Above we addressed the internal electron-hole motion in a localized immobile EH dimer resulting in an s-p splitting. However, the EH dimer can move in three-dimensional (3D) lattice thus developing new translational and rotational modes. For simplicity, hereafter we address an ideal cubic perovskite lattice where the main modes are rotations of the hole (electron) around the electron (hole) by 90° and 180° and axial translations. It is interesting to note that the 90° and 180° rotations of the hole (electron) around the electron (hole) correspond to the next-nearest-neighbor (NNN) and next-next-nearest-neighbor (NNNN) hoppings of the hole (electron) MnO_6^{8-} (MnO_6^{10-}) center in the lattice formed by the MnO_6^{9-} centers. We can introduce a set of transfer parameters to describe the dimer dynamics

$$t_s = -t_p \approx \frac{1}{2}(t^e_{\mathrm{NNNN}} + t^h_{\mathrm{NNNN}}),$$

$$t_{sp} = -t_{ps} \approx \frac{1}{2}(t^e_{\mathrm{NNNN}} - t^h_{\mathrm{NNNN}})$$

for the collinear exciton motion and

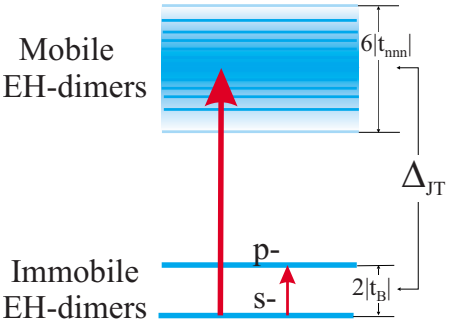

FIG. 5. (Color online) Schematic energy spectrum of immobile (localized) and mobile EH dimers. Bold arrows point to allowed electrodipole transitions.

$$t_s^{xy} = -t_p^{xy} \approx \frac{1}{2}(t_{\mathrm{NNN}}^e + t_{\mathrm{NNN}}^h),$$

$$t_{sp}^{xy} = t_{ps}^{xy} \approx \frac{1}{2}(t_{\mathrm{NNN}}^e - t_{\mathrm{NNN}}^h),$$

corresponding to a 90° rotation ($x \rightarrow y$ motion) of the exciton. All these parameters have a rather clear physical sense. The electron (hole) transfer integrals for collinear exciton transfer $t_{\mathrm{NNNN}}^{e,h}$ are believed to be smaller than $t_{\mathrm{NNN}}^{e,h}$ integrals for rectangular transfer. In other words, the two-center dimers prefer to move "crablike" rather than in the usual collinear mode. This implies a large difference for the dimer dispersion in [100] and [110] directions.

The motion of the EH dimer in the bare $LaMnO_3$ lattice with the orbital order of the Jahn-Teller Mn^{3+} ions bears an activation character with an activation energy $\Delta E = \frac{1}{2}\Delta_{\mathrm{JT}}$, where Δ_{JT} is the Jahn-Teller splitting of the e_g levels in Mn^{3+} ions. Thus one may conclude that the EH-dimer energy band in the bare $LaMnO_3$ lattice would be composed of the low-energy subband of immobile localized EH dimers or *sp* doublet with the energy separation of $2|t_B|$ and the high-energy subband of mobile EH dimers shifted by $\frac{1}{2}\Delta_{\mathrm{JT}}$ with the bandwidth $W \sim 6t_{\mathrm{NNN}}$, where t_{NNN} is an effective next-nearest-neighbor $e_g - e_g$ transfer integral in Mn^{3+}-Mn^{3+} pair. Schematically the spectrum is shown in Fig. 5. An optical portrait of the EH-dimer bands is composed of a rather narrow low-energy line due to electrodipole CT *s-p* transition for immobile dimers peaked at $E_{sp} = 2|t_B|$ and a relatively broad high-energy line due to electrodipole photoinduced dimer transport peaked at $E \approx \frac{1}{2}\Delta_{\mathrm{JT}} + |t_B|$. To estimate these energies one might use our aforementioned estimates for $|t_B| \approx 0.03$ eV and reasonable estimates of the Jahn-Teller splitting $\Delta_{\mathrm{JT}} \approx 0.7$ eV (see, e.g., Ref. 34). Thus we predict a two-peak structure of the EH-dimer optical response with a narrow line at ~0.06 eV and a broad line at ~0.4 eV. Our estimate of the *sp*-separation $E_{sp} = 2|t_B|$ does not account for the Jahn-Teller polaronic effects in the EH dimer that can result in its strong increase.

It is worth noting that the activation character for the motion of the EH dimer in parent manganite lattice implies the same feature for the generic 2 eV *d-d* CT exciton resulting in its weak dispersion. Indeed, the resonant inelastic x-ray scattering (RIXS) experiments on parent manganite $LaMnO_3$ by Inami *et al.*[51] found the energy dispersion of the 2.0–2.5 eV peak to be less than a few hundred meV.

D. EH dimers: EH dissociation and recombination.

The EH-dimer dissociation or uncoupling energy may be estimated to be on the order of 1.0–1.5 eV. The EH coupling within the dimer is determined by a cumulative effect of electrostatic attraction and local lattice relaxation (reorganization) energy.

The EH recombination in the EH dimer resembles an inverse disproportionation reaction,

$$\mathrm{MnO_6^{8-}} + \mathrm{MnO_6^{10-}} \rightarrow \mathrm{MnO_6^{9-}} + \mathrm{MnO_6^{9-}}. \qquad (15)$$

The inverse counterpart of 2 eV *d-d* CT transition in the bare parent manganite is expected to have nearly the same energy. CT transition (15) in EH dimer can be induced only in $\mathbf{E} \| \mathbf{R}_{\mathrm{MnMn}}$ polarization. However, this CT transition can be hardly photoinduced from the ground *s*-type state of the EH dimer in contrast with the *p*-type state due to selection rules for electrodipole transitions. It means that at least at rather low temperatures $kT \ll 2|t_B|$ the EH recombination band would be invisible; that is, the optical response of EH dimers would be reduced to two aforementioned low-energy bands that are developed within the energy gap of the bare parent manganite. In addition, we should point to different *p-d* CT transitions within electron $\mathrm{MnO_6^{10-}}$ and hole $\mathrm{MnO_6^{8-}}$ centers with the onset energy near 3 eV. It is worth noting that the overall optical response of the EH dimers in weakly distorted perovskite lattice is expected to be nearly isotropic at variance with the CT response of parent $LaMnO_3$ in its bare A-AFI phase.[34]

V. ELECTRON-HOLE BOSE LIQUID: THE TRIPLET BOSON DOUBLE-EXCHANGE MODEL

A. Effective Hamiltonian

To describe the electron-hole Bose liquid (EHBL) phase that evolves from EH dimers we restrict ourselves with orbital singlets ${}^6A_{1g}$ and ${}^4A_{2g}$ for the electron $\mathrm{MnO_6^{10-}}$ and hole $\mathrm{MnO_6^{8-}}$ centers, respectively. Specific electron configurations of these centers, $t_{2g}^3; {}^4A_{2g} e_g^2; {}^3A_{2g}: {}^6A_{1g}$ and $t_{2g}^3; {}^4A_{2g}$, respectively, enable us to consider the electron center $\mathrm{MnO_6^{10-}}$ to be composed of the hole $\mathrm{MnO_6^{8-}}$ center and a two-electron $e_g^2; {}^3A_{2g}$ configuration which can be viewed as a composite triplet boson. In the absence of the external magnetic field the effective Hamiltonian of the electron-hole Bose liquid takes the form of the Hamiltonian of the quantum lattice Bose gas of the triplet bosons with an exchange coupling,

$$\hat{H} = \hat{H}_{\mathrm{QLBG}} + \hat{H}_{\mathrm{ex}} = \sum_{i \neq j,m} t_B(ij) \hat{B}_{im}^{\dagger} \hat{B}_{jm} + \sum_{i>j} V_{ij} n_i n_j - \mu \sum_i n_i + \sum_{i>j} J_{ij}^{hh} (\hat{\mathbf{S}}_i \cdot \hat{\mathbf{S}}_j) + \sum_{i \neq j} J_{ij}^{hb} (\hat{\mathbf{s}}_i \cdot \hat{\mathbf{S}}_j) + \sum_{i>j} J_{ij}^{bb} (\hat{\mathbf{s}}_i \cdot \hat{\mathbf{s}}_j) + \sum_i J_{ii}^{hb} (\hat{\mathbf{s}}_i \cdot \hat{\mathbf{S}}_j). \qquad (16)$$

Here $\hat{B}^{\dagger}_{im}$ denotes the $S=1$ boson creation operator with a spin projection m at the site i and $\hat{B}_{im}$ is a corresponding annihilation operator. The boson number operator $\hat{n}_{im}=\hat{B}^{\dagger}_{im}\hat{B}_{im}$ at i site due to the condition of the on-site infinitely large repulsion $V_{ii}\rightarrow+\infty$ (*hardcore boson*) can take values 0 or 1.

The first term in Eq. (16) corresponds to the kinetic energy of the bosons; $t_B(ij)$ is the transfer integral. The second one reflects the effective repulsion ($V_{ij}>0$) of the bosons located on the neighboring sites. The chemical potential μ is introduced to fix the boson concentration: $n=\frac{1}{N}\Sigma_i\langle\hat{n}_i\rangle$. For EHBL phase in parent manganite we arrive at the same number of electron and hole centers, that is, to $n=\frac{1}{2}$. The remaining terms in Eq. (16) represent the Heisenberg exchange interaction between the spins of the hole centers (term with J^{hh}), spins of the hole centers and the neighbor boson spins (term with J^{hb}), boson spins (term with J^{bb}), and the very last term in Eq. (16) stands for the intracenter Hund exchange between the boson spin and the spin of the hole center. In order to account for the Hund rule one should consider J^{hb}_{ii} to be infinitely large ferromagnetic. Generally speaking, this model Hamiltonian describes the system that can be considered as a Bose analog of the *one orbital* double-exchange model system.[2]

Aforementioned estimates for different superexchange couplings given the bond geometry typical for $LaMnO_3$ predict antiferromagnetic coupling of the nearest-neighbor (NN) hole centers ($J^{hh}>0$), antiferromagnetic coupling of the two nearest-neighbor bosons ($J^{bb}>0$), and ferromagnetic coupling of the boson and the nearest-neighbor hole centers ($J^{hb}<0$). In other words, we arrive at highly frustrated system of triplet bosons moving in a lattice formed by hole centers when the hole centers tend to order G-type antiferromagnetically; the triplet bosons tend to order ferromagnetically both with respect to its own site and its nearest neighbors. Furthermore, nearest-neighboring bosons strongly prefer an antiferromagnetic ordering. Lastly, the boson transport prefers an overall ferromagnetic ordering.

B. Implications for phase states and phase diagram

By now we have no comprehensive analysis of phase states and phase diagram for the generalized triplet boson double-exchange model. The tentative analysis of the model in framework of a mean-field approximation (MFA) (Ref. 52) allows us to predict a very rich phase diagram even at half-filling ($n=\frac{1}{2}$) with a rather conventional diagonal long-range order (DLRO) with ferromagnetic insulating or ferromagnetic metallic (FM) phase and unconventional off-diagonal long-range order (ODLRO) with a coexistence of superfluidity of triplet bosons and ferromagnetic ordering. However, it is unlikely that the MFA approach can provide a relevant description of such a complex system. Some implications may be formulated from the comparison with familiar double-exchange model,[2] singlet boson Hubbard model (see, e.g., Ref. 53), and with generic bismuthate oxide $BaBiO_3$ as a well documented disproportionated system which can be described as a 3D system of the spin-singlet local bosons.

If the boson transfer is excluded we arrive at a spin system resembling that of mixed orthoferrite-orthochromite $LaFe_{1-x}Cr_xO_3$ [$n_B=\frac{1}{2}(1-x)$] which is a G-type antiferromagnet all over the dilution range $0<x<1$ with T_N's shifting from $T_N=740$ K for $LaFeO_3$ to $T_N=140$ K for $LaCrO_3$.[54] However, at variance with a monovalent (Fe^{3+}-Cr^{3+}) orthoferrite-orthochromite the Mn^{2+}-Mn^{4+} charge system in the EHBL phase would reveal a trend to a charge ordering, e.g., of a simple checkerboard G type in $LaMnO_3$ ($n_B=\frac{1}{2}$). It is worth noting that the naively expected large values of a boson-boson repulsion V_{ij} would result in a large temperature T_{CO} of the charge ordering well beyond room temperature. However, the manganites must have a large dielectric function and a strong screening of the repulsion; hence moderate values of V_{NN} and T_{CO}'s predicted.

However, such a scenario breaks when the boson transport is at work. It does suppress both types of charge and spin ordering and we arrive most likely at an inhomogeneous system with a glasslike behavior of charge and spin subsystems, which does or does not reveal a long-range ferromagnetic order at low temperatures. A question remains: whether the EHBL Hamiltonian (16) can lead to uniform solutions beyond MFA?

According to experimental data[19] the phases in $LaMnO_3$, which we relate with EHBL, exhibit a long-range ferromagnetic order below $T_C\approx140$ K, however, with rather small values of a mean magnetic moment, which agrees with a spin inhomogeneity. It is worth noting that the glass scenario implies a specific "freezing" temperature T_g to be a remnant of the MFA critical temperature. Such a temperature should be revealed in physical properties of the system.

With a deviation from half-filling to $n_B<\frac{1}{2}$ the local triplet bosons gain in freedom to move and improve their kinetic energy. On the other hand it is accompanied by a sharp decrease in the number of the boson-boson pairs with the most strong e_g-e_g antiferromagnetic coupling. In other words, a FM phase becomes a main candidate to a ground state.

Interestingly, that an intent reader can note that here we describe main features of phase diagrams typical for hole doped manganites such as $La_{1-x}Ca_xMnO_3$. Indeed, this resemblance seems not to be accidental one and points to a profound role of the EHBL phase in unconventional properties of doped manganites as well.

One of the most intriguing and challenging issues is related with the probable superfluidity of the triplet local bosons. Indeed, the boson transfer integral t_B defines a maximal temperature $T_{max}\approx t_B$ of the onset of local superconducting fluctuations in the hardcore boson systems.[55] Our estimations point to $T_{max}\approx300-700$ K, where the lower bound is taken from theoretical estimations, while the upper bound is derived from optical data on the 0.1 eV spectral feature. However, these high values of T_{max} do not give rise to optimistic expectations regarding the high-T_c bulk superconductivity in the EHBL phase of parent manganites first because of a spin frustration. Nevertheless, despite the fact that the emergence of a bulk superconductivity in a highly frustrated multicomponent EHBL phase seems to be a very uncommon phenomenon, the well-developed local superconducting fluctuations can strongly influence the transport as well as other physical properties. A detailed analysis of the bosonic

double-exchange model, in particular, of the off-diagonal superconducting order with the superfluidity of the triplet local bosons remains to be a challenging issue for future studies. It is worth noting that the electron-lattice coupling can be strongly involved into the buildup of the electronic structure of the bosonic double-exchange model, in particular, strengthening the EH-dimer fluctuations.

VI. EXPERIMENTAL MANIFESTATION OF EH DROPLETS IN PARENT AND LOW-HOLE-DOPED MANGANITES

Above, in Sec. II we addressed some experimental data that somehow pointed to a disproportionation scenario and have been used to start with a detailed analysis of the EHBL phase. Hereafter, we address different new experimental data that support our scenario in some details.

A. Optical response of electronically phase-separated manganites

The CT unstable systems will be characterized by a well-developed volume fraction of the short- and long-lived CT excitons or the EH droplets that can give rise to a specific optical response in a wide spectral range due to different *p-d* and *d-d* CT transitions. First, these are the low-energy intra-center CT transitions and high-energy inverse *d-d* CT transitions, or EH recombination process in EH dimers and/or nanoscopic EH centers, and different high-energy CT transitions in electron and hole centers. It is worth noting that, strictly speaking, the optical measurements should always display a larger volume fraction of EH droplets as compared with static or quasistatic measurements because these "see" short-lived droplets as well. What are the main optical signatures of the CT instability? A simplified picture implies the spectral weight transfer from the bare CT band to the CT gap with an appearance of the midgap bands and smearing of the fundamental absorption edge. Such a transformation of the optical response is shown schematically in Fig. 6. The transferred spectral weight can be easily revealed in the spectral window of the bare insulator to be a direct indicator of the CT instability. It is worth noting that the fragile "matrix-droplet " structure of the parent manganites makes the optical response to be very sensitive to such factors as temperature, sample shape (bulk crystal, thin film) and quality, and external magnetic field, which can explain some inconsistencies observed by different authors (see, e.g., Refs. 34 and 56–58). Great care is needed if one wants to separate off the volume fraction effects to obtain the temperature behavior of spectral weight for certain band and compare the results with those observed by different groups on different samples. Charge transfer instability and the CT exciton self-trapping in nominally pure manganites are indeed supported by the studies of their optical response.

Anisotropic optical conductivity spectra for a detwinned single crystal of $LaMnO_3$, which undergoes the orbital ordering below $T_{JT} \approx 780$ K, have been derived from the reflectivity spectra investigated by Tobe *et al.*[56] over a wide temperature range, $10\ \mathrm{K} < T < 800\ \mathrm{K}$ (see Fig. 7). As

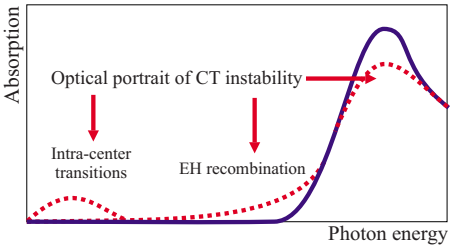

FIG. 6. (Color online) Optical response (schematically) of the self-trapped CT excitons and EH droplets (dotted curves). Arrows point to a spectral weight transfer from the bare CT band to the CT gap with an appearance of the midgap bands and/or smearing of the fundamental absorption edge.

temperature is increased, the EH dimers generating *d-d* CT transition peaked around 2 eV show a dramatic loss of spectral weight with its partial transfer to the low energies. Simultaneously one observes a suppression of optical anisotropy. Above T_{JT}, the gap feature becomes obscure and the anisotropy disappears completely. Such a behavior of the 2 eV band can be hardly explained by the effect of spin fluctuations,[34] most likely it points to a shrinking of the A-AFI phase volume fraction with approaching to $T_{disp} = T_{JT}$ and phase transition to an unconventional metallicklike phase. However, the optical conductivity does not reveal any signatures of Drude peak, which together with a rather large resistivity[9] points to an unusual charge transport.

Main features of the optical response[56] agree with predictions followed from the EPS phase diagram and isotropic character of the optical response of EH droplets. However, the reflectivity data did not reveal any midgap structures which observation and identification needs usually in direct absorption/transmission measurements. The most detailed studies of spectral, temperature, and doping behavior of the midgap bands were performed in Refs. 58–62. All the manganites investigated, both parent and hole/electron doped, show up two specific low-energy optical features peaked near 0.10–0.15 eV (0.1 eV band) and 0.3–0.6 eV (0.5 eV band). Results of the ellipsometric and direct absorption measurements for a single-crystalline parent $LaMnO_3$ sample are shown in Fig. 8; these directly reveal both 0.1 and 0.5 eV

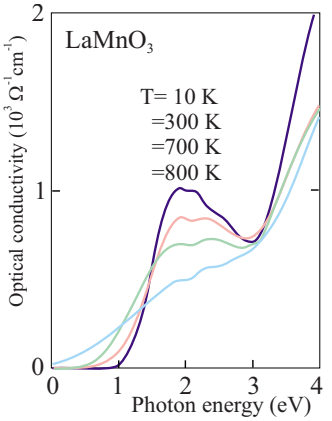

FIG. 7. (Color online) Temperature dependence of optical conductivity of parent $LaMnO_3$ for $\mathbf{E} \| \mathbf{ab}$ (reproduced from Ref. 56).

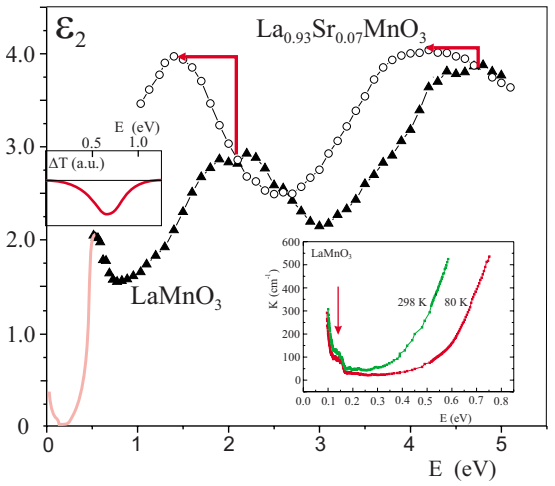

FIG. 8. (Color online) Imaginary part of the dielectric function ε_{ab} in $LaMnO_3$ (solid triangles) and $La_{0.93}Sr_{0.07}MnO_3$ (open circles) (Ref. 58). Low-energy part of the spectrum is a guide for eyes from the infrared absorption data (see right-hand inset). Right-hand inset: infrared absorption for parent $LaMnO_3$ at 80 and 298 K (reproduced from Ref. 58). Left-hand inset: photoinduced transmittance of parent $LaMnO_3$ at $T=25$ K (reproduced from Ref. 10).

features in the spectral window of the bare matrix.[58] These two bands can be naturally attributed to the CT transitions within the immobile EH dimers and to the dimer transport activating transitions, respectively. Respective energies agree with theoretical predictions, although more accurate value of 0.15 eV for the "0.1 eV" peak points most likely to an essential electron-lattice effect.

The 0.5 eV band in $LaMnO_3$ was revealed by photoinduced absorption spectroscopy under light excitations with the photon energy near 2.4 eV that provides optimal conditions for the EH-pair creation. Photoinduced absorption was observed[10] with a strong broad midinfrared peak centered at ~ 5000 $cm^{-1} \approx 0.62$ eV. Since the laser photoexcitation and measurement are pseudocontinuous, the photoexcited EH-pair lifetimes need to be quite long for any significant photoexcited EH-pair density to build up. It means that the lattice is arranged in the appropriate relaxed state. The origin of the photoinduced (PI) absorption peak was attributed[10] to the photon-assisted hopping of anti-Jahn-Teller polarons formed by photoexcited charge carriers. This interpretation was based on the assumption of primary p-d CT transition induced by excitation light with the energy $h\nu=2.41$ eV. However, the d-d CT transition nature of 2 eV absorption band in $LaMnO_3$ (Ref. 34) unambiguously points to the EH dimers to be main contributor to PI absorption peak. In such a case, the PI absorption peak energy (~ 0.6 eV) may be attributed to the energy of the photon-assisted hopping of the relaxed EH dimers (see Fig. 5) and can be used as an estimate of the Jahn-Teller energy Δ_{JT}.

Similarly, so-called midgap features in nominally pure manganites were directly or indirectly observed by many authors. Furthermore, it seems that some authors did not report the optical data below 1.5 eV to avoid the problems with these odd features. Observation of the MIR features agrees with the scenario of well-developed intrinsic electronic inhomogeneity inherent to nominally stoichiometric insulating manganites and composed of volume fraction of conceivably EH droplet phase.

Finally, it is instructive to compare the midgap absorption spectrum of parent manganite with IR optical spectra of chemically doped compounds to see whether the nonisovalent substitution stimulates the condensation of EH pairs and respective rise of the EH droplet volume fraction. Indeed, Okimoto *et al.*[63] observed in $La_{0.9}Sr_{0.1}MnO_3$ a broad absorption peaked around 0.5 eV which is absent at room temperature and increases in intensity with decreasing temperature. In addition, the absorption feature reported also shifts to lower energy as doping is increased, in agreement with PI measurements.[10] A midgap state with a similar peak energy and similar doping dependence was also observed at room temperature by Jung *et al.*[64] in $La_{1-x}Ca_xMnO_3$.

Thus we see that the strong and broad midinfrared optical feature peaked near 0.5 eV and observed in all the perovskite manganites studied can be surely attributed to the optical response of isolated EH dimers or small EH droplets edged by the JT Mn^{3+} centers, more precisely, to an optical activation of the dimer transport in such a surroundings. The peak energy may be used to estimate the Jahn-Teller splitting for e_g levels in Mn^{3+} centers and its variation under different conditions.

B. Lattice effects in parent $LaMnO_3$

The unusual abrupt unit-cell volume contraction by 0.36% has been observed by Chatterji *et al.*[65] in $LaMnO_3$ at T_{JT}. The high-temperature phase just above T_{JT} has less volume than the low-temperature phase.

The local structure of stoichiometric $LaMnO_3$ across the Jahn-Teller transition at T_{JT} was studied by means of extended x-ray absorption fine structure (EXAFS) at Mn K edge[66] and high real space resolution atomic pair distribution function (PDF) analysis.[67] Both techniques reveal two different Mn-O separations, 1.92 Å (1.94 Å) and 2.13 Å (2.16 Å), distributed with intensity 2:1, respectively. Comparing these separations with room-temperature neutron-diffraction data[21] (1.907, 1.968, and 2.178 Å) both groups point to a persistence of the JT distortions of MnO_6 octahedra on crossing T_{JT}. However, both this result and that of Chatterji *et al.*[65] most likely point to a transition to Mn-O separations specific for EH dimers or nearest-neighbor electron $MnO_6^{10-}(Mn^{2+})$ and hole $MnO_6^{10-}(Mn^{4+})$ centers coupled by fast electron exchange. In any case the picture is that in the high-temperature O phase the local distortions of the Mn-O separations are dynamical in character similar to those in $BaBiO_3$. A signature of that is an excess increase in the thermal factors of oxygen atoms in going from O′ to the O phase.[17] The observed Raman spectra for undoped $LaMnO_3$ crystal at ambient pressure and room temperature reveal a number of additional lines, in particular, strong $(A_{1g}+B_{2g})$ mode 675 cm^{-1}, which are also have been observed in the spectra of doped materials and may be attributed to droplets of EHBL phase.[68]

Strong variation in the $LaMnO_3$ Raman spectra, both of intensity and energy shift with increasing laser power,[69]

could be related to the photoinduced nucleation and the volume expansion of the EH Bose liquid. Surely, laser annealing can simply increase the temperature thus resulting in an A-AFI/EHBL volume fraction redistribution. The strong variations in the $LaMnO_3$ Raman spectra on the excitation laser power provide evidence for a structural instability that may result in a laser-irradiation-induced structural phase transition. It is worth noting a strong resonant character of the excitation of the Raman specta[70] that points to a need in more extensive studies focused on the search of the EH droplet response.

The intrinsic electronic phase separation inherent for nominally undoped stoichiometric $LaMnO_3$ manifests itself in remarkable variations in x-ray diffraction pattern, optical reflectivity and Raman spectra, and resistivity under pressures up to 40 GPa.[11] The pressure-induced variations in Raman spectra, in particular, a blueshift and the intensity loss of the in-phase O2 stretching B_{2g} mode with a concomitant emergence of a peak at ~ 45 cm^{-1} higher in energy evidenced some kind of electronic phase separation with a steep rise of the volume fraction of the domains of a phase within the parent A-AFI phase ("sluggish" transition[11]). Evolution of phase was accompanied by a dramatic change in reflectance which resembles that of $LaMnO_3$ at ambient pressure on heating from low temperatures to $T > T_{JT}$.[56] Furthermore, the system exhibited an anomalously strong pressure-induced fall of the room-temperature resistivity by 3 orders of magnitude in the range of 0–30 GPa with an IM transition at 32 GPa. An overall fall of resistivity in the range of 0–32 GPa amounts to 5 orders of magnitude. However, the system retains a rather high resistance, exhibiting a "poor" metallic behavior typical for EHBL phase. It is worth noting that at high pressures >30 GPa the resistivity does not reveal sizable temperature dependence between 80 and 300 K similarly to the high-temperature $T > T_{JT}$ behavior of $LaMnO_3$ at ambient pressure (see Ref. 9 and Fig. 1). Overall these data provide a very strong support for our scenario of the A-AFI/EHBL electronic phase separation in parent manganite taking place without any hole/electron doping.

The effect of the $O^{16} \rightarrow O^{18}$ isotope substitution on the IM transition and optical response[71] can be easily explained as a result of an energy stabilization of the parent A-type antiferromagnetic phase as compared with the EH Bose liquid. The percolation mechanism of the isotope effect in manganites is considered in Ref. 71.

C. Magnetic and resonance properties of EHBL phase in $LaMnO_3$

What about the magnetic properties of the phase? In the framework of our scenario the EH Bose liquid in $LaMnO_3$ evolves from the EH dimers which are peculiar magnetic centers with intrinsic spin structure and with enormously large magnetic moments in their ground ferromagnetic state. However, the EH dimers exist as well defined entities only at very initial stage of the EHBL evolution. Within well-developed EH Bose liquid we deal with a strong overlap of EH dimers when these lose individuality. A tentative analysis of the EH liquid phase in parent manganites[26] shows that it may be addressed to be a triplet bosonic analog of a simple fermionic double-exchange model with a well-developed trend to a ferromagnetic ordering. It is interesting that both models have much in common that hinders their discerning. In both cases the net magnetic moment of calcium (strontium)-doped manganite $La_{1-x}Ca(Sr)_xMnO_3$ saturates to the full ferromagnetic value $\approx (4-x)\mu_B$/f.u. Well developed ferromagnetic fluctuations within EHBL phase in $LaMnO_3$ have been observed in high-temperature susceptibility measurements by Zhou and Goodenough[9] which measured the temperature dependence of paramagnetic susceptibility both below and above T_{JT}. They observed a change from an anisotropic antiferromagnetism to an isotropic ferromagnetism crossing T_{JT} accompanied by an abrupt rise of magnetic susceptibility. These data point to an energy stabilization of the EH Bose liquid in an external magnetic field as compared with a parent A-type antiferromagnetic phase.

The dc magnetic susceptibility shows two distinct regimes[72,73] for $LaMnO_3$, above and below T_{JT}. For $T > T_{JT}$, $\chi_{dc}(T)$ follows a Curie-Weiss (CW) law, $\chi_{dc}(T) = C/(T-\Theta)$, with $C = 3.4$ emu K/mol ($\mu_{eff} \approx 5.22\mu_B$) and $\Theta \approx 200$ K. For $T < T_{JT}$ the behavior of magnetic susceptibility strongly depends on the samples studied. Zhou and Goodenough[9] observed an abrupt fall in the Weiss constant on crossing T_{JT} from large ferromagnetic to a small antiferromagnetic $\Theta \approx 50$ K, while Causa and co-workers[72,73] found that the Curie-Weiss behavior of $\chi_{dc}(T)$ is recovered only near room temperature with a reduced antiferromagnetic $\Theta \approx 75$ K. Interestingly that instead of a natural suggestion of an electronic phase-separated state below T_{JT} with a coexistence of low- and high-temperature phases and steep change in effective Θ, the authors[72,73] explained their data as a manifestation of dramatic changes in exchange parameters induced by crystal distortions. They refer to theoretical calculations[74] which show that J_{ab} in parent manganites is FM and decreases with the JT distortion while J_c changes from FM in the pseudocubic O phase to AFM in the O′ phase. However, the aforementioned estimations[46] based on the experimental data for isostructural orthoferrites, orthochromites, and mixed orthoferrites chromites point to a more reasonable antiferromagnetic orbitally averaged exchange coupling of two Mn^{3+} ions with bond geometry typical for $LaMnO_3$: $J \approx 12.6$ K.

Magnetic measurements for low-hole-doped $LaMnO_3$ samples[75–79] reveal a coexistence of antiferromagnetic matrix with ferromagnetic clusters or spin-glass behavior, accompanied by magnetic hysteresis phenomena. Anomalous magnitudes of the effective magnetic moment per manganese ion that considerably exceed expected theoretical values, up to $\mu_{eff} \approx 6\mu_B$ in $La_{0.9}Sr_{0.1}MnO_3$ (Ref. 76), were explained to be an evidence of a disproportionation $2Mn^{3+} \rightarrow Mn^{4+} + Mn^{2+}$ (Ref. 75) or a superparamagnetic behavior of ferromagnetic clusters.[76] As a whole, magnetic measurements for nearly stoichiometric $LaMnO_3$ support the disproportionation scenario.

The electronic spin resonance (ESR) spectrum of $LaMnO_3$ in a wide temperature range above T_N and up to temperature ~ 800 K above T_{JT} shows a single Lorentzian line with $g \sim 1.98-2.00$ and $\Delta H \sim 2400$ Gauss at room temperature.[72,80] In common, the spectrum intensity follows

the dc susceptibility; however, the consistent interpretation of the origin of ESR signal, especially in O pseudocubic phase, is still lacking. Two different electronic phases are documented by ESR measurements in slightly La-deficient $La_{0.99}MnO_3$.[79] Further experimental ESR studies have to be carried out to clarify the issue.

The ^{55}Mn nuclear magnetic resonance (NMR) data support most likely the EHBL scenario. Indeed, the zero-field ^{55}Mn NMR spectrum in a nominally undoped $LaMnO_3$ consists of a sharp central peak at 350 MHz due to bare $Mn^{3+}O_6^{9-}$ centers and two minority signals at approximately 310 and 385 MHz,[48] which can be assigned to a localized hole $MnO_6^{8-}(=Mn^{4+})$ center and EH dimers with a fast bosonic exchange, respectively. Evolution of such a picture with Ca(Sr) doping can easily explain a complex ^{55}Mn NMR line shape in $La_{1-x}Ca(Sr)_xMnO_3$ samples.[48,77] It is worth noting that Tomka *et al.*[47] observed three ^{55}Mn NMR signals in a hole doped $PrMnO_3$ around 310, 400, and 590 MHz, which can be attributed to localized hole MnO_6^{8-} and electron MnO_6^{10-} centers (narrow resonances around 310 and 590 MHz, respectively) and to EH droplets with a fast bosonic exchange (broad resonance around 400 MHz).

It is worth noting that the ^{55}Mn NMR line shape in $La_{1-x}Ca(Sr)_xMnO_3$ samples[48,77] with a most part of intensity shifted to a very broad line in the range of 350–450 MHz can hardly be explained in framework of a so-called double-exchange (DE) line[48] with a frequency $f_{DE}=\frac{1}{2}[f(Mn^{3+})+f(Mn^{4+})]$ derived from that typical for Mn^{3+} (350 MHz) and Mn^{4+} (310 MHz). Our scenario with a broad line centered with more or less redshift from a frequency specific for a high-spin state of the EH dimer: $f_{EH}=\frac{1}{2}[f(Mn^{2+})+f(Mn^{4+})]\approx 450$ MHz with $f(Mn^{2+})\approx 590$ MHz and $f(Mn^{4+})\approx 310$ MHz is believed to be more appropriate one. It is worth noting that the ^{55}Mn NMR response of EH dimers can shed some light on several ^{55}Mn NMR puzzles, in particular, observation of the low-temperature (4.2 K) low-frequency NMR lines at 260 MHz in one of nominally undoped $LaMnO_3$ samples[81] and even at 100 MHz in a more complex manganite $(BiCa)MnO_3$.[49] In both cases we deal seemingly with a some sort of a stabilization of low-spin states for EH dimers, for instance, due to the Mn-O-Mn bond geometry distortions resulting in an antiferromagnetic Mn^{2+}-O-Mn^{4+} superexchange.

The ^{55}Mn NMR spectra of slightly nonstoichiometric $LaMnO_3$ (Ref. 50) may be viewed as the most striking evidence of the EH-dimer response in a spin inhomogeneous glasslike state. A simple comparison of experimental spectra with theoretical predictions for EH dimers (see Fig. 4) shows a clear manifestation of the $S=4,3,2$ spin multiplets of the EH dimers with the mixing effects due to a spin noncollinearity.

Magnetic and transport properties of a single-crystalline parent undoped manganite $LaMnO_3$ have been studied recently under ultrahigh mega-Gauss magnetic field at helium temperatures.[13] In accordance with theoretical predictions[82] a sharp magnetic spin-flip transition was observed at about 70 T without visible transport anomalies. On further rising the magnetic field the authors observed unusual magnetoinduced IM transition at $H_{IM}\sim 220$ T that is considerably above the field of the magnetic saturation of the A-AFI phase. Large values of the *p-d* or *d-d* charge transfer energies in bare A-AFI phase of parent manganites [~ 2 eV in $LaMnO_3$ (Ref. 34)] make the energy difference between the A-AFI ground state and any metallic phase seemingly too large to be overcome even for magnetic fields as large as hundreds of tesla. Zeeman energy associated with such a field is clearly more than 1 order of magnitude smaller than the charge reordering energy. Thus we see that a puzzling field-driven IM transition cannot be explained within a standard scenario implying the parent manganite $LaMnO_3$ to be a uniform system of the Jahn-Teller Mn^{3+} centers with an *A*-type antiferromagnetic order and needs a revisit of our view on the stability of its ground state. However, our scenario can easily explain the puzzling field-driven IM transition in perovskite manganite $LaMnO_3$ (Ref. 13) to be a result of a percolative transition in an inhomogeneous phase-separated A-AFI/EHBL state. The volume fraction of the ferromagnetic EHBL phase grows in an applied magnetic field, and at a sufficiently high field this fraction reaches its percolation threshold to give the IM transition. It is clear that a relatively small zero-field volume fraction of ferromagnetic EHBL phase in the parent manganite has required large magnetic field to induce the IM transition.

D. Dielectric anomalies in $LaMnO_3$

The broadband dielectric spectroscopy helps in characterizing the phase states and transitions in Mott insulator. Above we pointed to anomalous electric polarizability of the EH dimers and EH droplets that would result in dielectric anomalies in the EHBL phase and the phase-separated state of $LaMnO_3$. Indeed, such anomalies were reported recently both for polycrystalline and single-crystalline samples of parent $LaMnO_3$. First of all, one should note relatively high static dielectric constant in $LaMnO_3$ at $T=0$ ($\varepsilon_0\sim 18-20$) approaching to values typical for genuine multiferroic systems ($\varepsilon_0\approx 25$), whereas for the conventional nonpolar systems, ε_0 varies within 1–5. The entire $\varepsilon'(\omega,T)-T$ pattern across 77–900 T has two prominent features: (i) near T_N and (ii) near T_{JT} to be essential signatures of puzzlingly unexpected multiferroicity. Far below T_N, $\varepsilon'(\omega,T)$ is nearly temperature and frequency independent, as expected. Following the anomaly at T_N, $\varepsilon'(\omega,T)$ rises with T by 5 orders of magnitude near T_{JT}. Finally, ε' becomes nearly temperature independent beyond T_{JT}. The *P-E* loop does not signify any ferroelectric order yet the time-dependence plot resembles the "domain-switching-like" pattern. The finite loop area signifies the presence of irreversible local domain fluctuations. From these results, it appears that the intrinsic electrical polarization probably develops locally with no global ferroelectric order. The nature of the anomaly at T_{JT} varies with the increase in Mn^{4+} concentration following a certain trend—from a sharp upward feature to a smeared plateau and then a downward feature to finally a rather broader downward peak.

The observation of an intrinsic dielectric response in globally centrosymmetric $LaMnO_3$, where no ferroelectric order is possible due to the absence of off-center distortion in MnO_6 octahedra, cannot be explained in frames of the con-

ventional uniform antiferromagnetic insulating A-AFI scenario and agrees with the electronic A-AFI/EHBL phase-separated state with a coexistence of nonpolar A-AFI phase and highly polarizable EHBL phase.

E. Comment on the experimental nonobservance of the EHBL phase in $LaMnO_3$

By now there has been no systematic exploration of exact valence and spin state of Mn in perovskite manganites. Using electron paramagnetic resonance (EPR) measurements Oseroff *et al.*[80] suggested that below 600 K in $LaMnO_3$ there are no isolated Mn atoms with valences of +2, +3, and +4; however they argued that EPR signals are consistent with a complex magnetic entity composed of Mn ions of different valences.

Park *et al.*[83] attempted to support the Mn^{3+}/Mn^{4+} model based on the Mn $2p$ x-ray photoelectron spectroscopy (XPES) and O $1s$ absorption. However, the significant discrepancy between the weighted Mn^{3+}/Mn^{4+} spectrum and the experimental one for given x suggests a more complex doping effect. Subias *et al.*[84] examined the valence state of Mn utilizing Mn K-edge x-ray absorption near edge spectra (XANES); however, a large discrepancy is found between experimental spectra given intermediate doping and appropriate superposition of the end members.

The valence state of Mn in Ca-doped $LaMnO_3$ was studied by high-resolution Mn $K\beta$ emission spectroscopy by Tyson *et al.*[85] No evidence for Mn^{2+} was claimed at any x values seemingly ruling out proposals regarding the Mn^{3+} disproportionation. However, this conclusion seems to be absolutely unreasonable one. Indeed, electron center MnO_6^{10-} can be found in two configurations with formal Mn valences Mn^{2+} and Mn^{1+} (not simple Mn^{2+}). In its turn, the hole center MnO_6^{8-} can be found in two configurations with formal Mn valences Mn^{4+} and Mn^{3+} (not simple Mn^{4+}). Furthermore, even the bare center MnO_6^{9-} can be found in two configurations with formal Mn valences Mn^{3+} and Mn^{2+} (not simple Mn^{3+}). So, within the model the Mn $K\beta$ emission spectrum for the Ca-doped $LaMnO_3$ has to be a superposition of appropriately weighted Mn^{1+}, Mn^{2+}, Mn^{3+}, and Mn^{4+} contributions (not simple Mn^{4+} and Mn^{3+}, as one assumes in Ref. 85). Unfortunately, we do not know the Mn $K\beta$ emission spectra for the oxide compounds with Mn^{1+} ions; however a close inspection of the Mn $K\beta$ emission spectra for the series of Mn oxide compounds with Mn valence varying from 2+ to 7+ (Fig. 2 in Ref. 85) allows us to uncover a rather clear dependence on valence and indicates a possibility to explain the experimental spectrum for Ca-doped $LaMnO_3$ [Fig. 4(a)] as a superposition of appropriately weighted Mn^{1+}, Mn^{2+}, Mn^{3+}, and Mn^{4+} contributions. Later[86] it has been shown that Mn L-edge absorption rather than that of K edge is completely dominated by Mn $3d$ states and, hence, is an excellent indicator of Mn oxidation state and coordination. Interestingly that the results of the x-ray absorption and emission spectroscopy in vicinity of the Mn L_{23} edge[87] provide a striking evidence of a coexistence of Mn^{3+} and Mn^{2+} valence states in a single-crystalline $LaMnO_3$.

This set of conflicting data together with a number of additional data[88] suggests the need for an in-depth exploration of the Mn-valence problem in this perovskite system. However, one might say, the doped manganites are not only systems with mixed valence but systems with indefinite valence, where we cannot, strictly speaking, unambiguously distinguish Mn species with either distinct valence state.

It seems, by now, that there are no techniques capable of direct and unambiguous detection of electron-hole Bose liquid. However, we do not see any sound objections against such a scenario that is shown to explain a main body of experimental data.

VII. HOLE DOPING OF PARENT MANGANITE

Evolution of the electronic structure of nominally insulating $3d$ oxides under a nonisovalent substitution as in $La_{1-x}^{3+}Sr_x^{2+}MnO_3$ remains one of the challenging problems in physics of strong correlations. A conventional model approach focuses on a hole doping and implies a change in the (quasi)particle occupation in the valence band or a hole localization in either cation $3d$ orbital or anion O $2p$ orbital or in a proper hybridized molecular orbital. However, in the $3d$ oxides unstable with regard to a charge transfer such as parent manganites one should expect just another scenario when the nonisovalent substituents do form the nucleation centers for the EH droplets thus provoking the first-order phase transition into an EH disproportionated phase with a proper deviation from a half-filling.

Conventional double-exchange model implies the manganese location of the doped hole and its motion in the lattice formed by nominal parent manganite.[2] However, by now there are very strong hints at oxygen location of doped holes. One might point to several exciting experimental results supporting the oxygen nature of holes in manganites. The first is a direct observation of the O $2p$ holes in the O $1s$ x-ray absorption spectroscopy measurements.[89] Second, Tyson *et al.*[85] in their Mn $K\beta$ emission spectra studies of the Ca-doped $LaMnO_3$ observed an "arrested" Mn-valence response to the doping in the $x<0.3$ range, also consistent with creation of predominantly oxygen holes. Third, Galakhov *et al.*[90] reported Mn $3s$ x-ray emission spectra in mixed-valence manganites and showed that the change in the Mn formal valency from 3 to 3.3 is not accompanied by any decrease in the Mn $3s$ splitting. They proposed that this effect can be explained by the appearance in the ground-state configuration of holes in the O $2p$ states. The oxygen location of the doped holes is partially supported by observation of anomalously large magnitude of saturated magnetic moments in ferromagnetic state for different doped manganites.[75,76]

Two oxygen-hole scenarios are possible. The first implies the hole doping directly to bare A-AFI phase of parent manganite. Given light doping we arrive at the hole trapping in potential wells created by the substituents such as Ca^{2+}, Sr^{2+}, or cation vacancies. This gives rise to evolution of hole-rich orbitally disordered ferromagnetic phase. The volume fraction of this phase increases with x, and ferromagnetic ordering within this phase introduces spin-glass behavior where the ferromagnetic phase does not percolate in zero magnetic field $H=0$; but growth of the ferromagnetic phase to beyond percolation in a modest field can convert the spin glass to a

bulk ferromagnetic insulator. On further increasing the hole doping the ferromagnetic metallic ground state is obtained with itinerant oxygen holes and degenerate e_g orbitals of Mn^{3+} ions.

In second scenario one proposes that doped holes trigger the phase transition to an "asymmetrically" disproportionated phase with nominal non-JT Mn^{2+} ions and oxygen holes that can form a band of itinerant carriers. This scenario implies that the doped holes simply change a hole band filling.

Both scenario imply an unconventional system with two, Mn $3d$ and O $2p$, unfilled shells. One should note that despite a wide-spread opinion the correlation effects for the oxygen holes can be rather strong. These could provide a coexistence of the two (manganese and oxygen) nonfilled bands.

Such a p-d model with ferromagnetic p-d coupling immediately explains many unconventional properties of the hole doped manganites. First of all, at low-hole content we deal with hole localization in impurity potential. Then, given further hole doping a percolation threshold occurs accompanied by insulator-anionic oxygen metal phase transition and ferromagnetic ordering both in oxygen and Mn sublattices due to a strong ferromagnetic Heisenberg pd exchange. However, it should be noted that ferromagnetic sign of pd exchange is characteristic of nonbonding p and d orbitals.

The oxygen-hole doping results in a strong spectral weight transfer from the intense O $2p$-Mn $3d$ CT transition bands to the O $2p$ band developed. The Mn^{3+} d-d transitions will gradually shift to the low energies due to a partial O $2p$ hole screening of the crystalline field. In a whole, optical data do not disprove the oxygen-hole scenario.

Despite many controversial opinions regarding the electronic structure of doped holes the current description of complex phase diagrams for doped manganites implies a well-developed phase separation with coexistence of bare antiferromagnetic and several ferromagnetic phases.[2,91] What is the role played by the EHBL phase inherent for parent manganites?

Hole doping of parent manganite is produced by a nonisovalent substitution as in $La_{1-x}Sr_xMnO_3$ or by an oxygen nonstoichiometry. The Sr^{2+} and Ca^{2+} substituents form effective trapping centers for the EH dimers and the nucleation centers for the EH Bose liquid. At a critical substituent concentration $x_c \approx 0.16$ one arrives at a percolation threshold[3] when the conditions for an itinerant particle hopping do emerge. Holes are doped into EH Bose liquid of parent $LaMnO_3$ similar to generic $BaBiO_3$ system only pairwise, transforming formally electron MnO_6^{10-} center to hole MnO_6^{8-} center. Similarly to $BaBiO_3$ doped hole centers form local composite bosons which shift the system from half-filling ($n_B = 1/2$).

It seems the EHBL phase addressed above appears to be an important precursor for a ferromagnetic metallic phase responsible for colossal magnetoresistance observed in doped manganites. Existence of such an intermediate "poor metallic" phase seems to be essential for a transformation of bare insulating A-AFI phase to a "good-metallic" phase under hole doping. Low-energy CT excitations typical for EHBL phase and well exhibited in optical response (see Figs. 7 and 8) give rise to a significant screening of electrostatic interactions and to a suppression of localization trend for doped charge carriers with their escape out of charge traps and the evolution of itineracy. This trend is well illustrated in Fig. 8, where the dielectric function ε_2 is shown both for parent and slightly hole doped $LaMnO_3$. We see a clear redshift both for low-energy (2 eV) d-d CT band and high-energy (4.5 eV) p-d CT band with a rise of intensity for both bands, particularly sharp for the 2 eV band. All these effects evidence the lowering of effective values for the charge transfer energies, which is a clear trend to "metallicity."

One of the intriguing issues is related with seemingly masked superconducting fluctuations in doped manganites and its relation to colossal magnetoresistance. Indeed, doped manganites reveal many properties typical for superconducting materials or, rather, unconventional superconductors such as cuprates. Kim[92] proposed the frustrated p-wave pairing superconducting state similar to the A_1 state in superfluid He-3 to explain the CMR, the sharp drop of resistivity, the steep jump of specific heat, and the gap opening in tunneling of manganese oxides. In this scenario, colossal magnetoresistance (CMR) is naturally explained by the superconducting fluctuation with increasing magnetic fields. This idea is closely related to the observation of anomalous proximity effect between superconducting YBaCuO and a manganese oxide, $La_{1-x}Ca_xMnO_3$ or $La_{1-x}Sr_xMnO_3$,[93] and also the concept of local superconductivity manifested by doped manganites.[94]

VIII. CONCLUSION

To summarize, we do assign anomalous properties of parent manganite $LaMnO_3$ to charge transfer instabilities and competition between insulating A-AFM phase and metallic-like dynamically disproportionated phase formally separated by a first-order phase transition at $T_{disp} = T_{JT} \approx 750$ K. We report a comprehensive elaboration of a so-called disproportionation scenario in manganites which was addressed earlier by many authors; however, by now it was not properly developed. The unconventional high-temperature phase is addressed to be a specific electron-hole Bose liquid rather than a simple "chemically" disproportionated $R(Mn^{2+}Mn^{4+})O_3$ phase. We arrive at highly frustrated system of triplet $(e_g^2)^3A_{2g}$ bosons moving in a lattice formed by hole Mn^{4+} centers when the latter tend to order G-type antiferromagnetically and the triplet bosons tend to order ferromagnetically both with respect to its own site and its nearest neighbors, nearest neighboring bosons strongly prefer an antiferromagnetic ordering. Lastly, the boson transport prefers an overall ferromagnetic ordering.

Starting with different experimental data we have reproduced a typical temperature dependence of the volume fraction of the high-temperature mixed-valence EHBL phase. New phase nucleates as a result of the CT instability and evolves from the self-trapped CT excitons or specific EH dimers, which seem to be a precursor of both insulating and metallic-like ferromagnetic phases observed in manganites. We present a detailed analysis of electronic structure, energy spectrum, optical, magnetic, and resonance properties of EH dimers. We argue that a slight nonisovalent substitution, pho-

toirradiation, external pressure, or magnetic field gives rise to an electronic phase separation with a nucleation or an overgrowth of EH droplets. Such a scenario provides a comprehensive explanation of numerous puzzling properties observed in parent and nonisovalently doped manganite $LaMnO_3$ including an intriguing manifestation of superconducting fluctuations.

We argue that the unusual ^{55}Mn NMR spectra of nonisovalently doped manganites $LaMnO_3$ may be addressed to be a clear signature of a quantum disproportionation and formation of EH dimers. Given the complex phase-separation diagram of this class of materials, the study of the nominally stoichiometric parent compound could give a deep insight into the physics governing the doped version of these manganese oxides. It would be important to verify the expectations of EHBL scenario by more extensive and goaled studies.

ACKNOWLEDGMENTS

I thank N. N. Loshkareva, Yu. P. Sukhorukov, K. N. Mikhalev, Yu. B. Kudasov, and V. V. Platonov for stimulating and helpful discussions. The work was supported by RFBR under Grants No. 06-02-17242, No. 07-02-96047, and No. 08-02-00633.

[1] T. Kimura, T. Goto, H. Shintani, K. Ishizaka, T. Arima, and Y. Tokura, Nature (London) **426**, 55 (2003).
[2] E. Dagotto, T. Hotta, and A. Moreo, Phys. Rep. **344**, 1 (2001).
[3] L. P. Gor'kov and V. Z. Kresin, Phys. Rep. **400**, 149 (2004).
[4] Y. Tokura, Rep. Prog. Phys. **69**, 797 (2006).
[5] K. Dörr, J. Phys. D **39**, R125 (2006).
[6] T. V. Ramakrishnan, J. Phys.: Condens. Matter **19**, 125211 (2007).
[7] R. Raffaelle, H. U. Anderson, D. M. Sparlin, and P. E. Parris, Phys. Rev. B **43**, 7991 (1991).
[8] M. F. Hundley and J. J. Neumeier, Phys. Rev. B **55**, 11511 (1997).
[9] J.-S. Zhou and J. B. Goodenough, Phys. Rev. B **60**, R15002 (1999); **68**, 144406 (2003).
[10] T. Mertelj, D. Kuscer, M. Kosec, and D. Mihailovic, Phys. Rev. B **61**, 15102 (2000).
[11] I. Loa, P. Adler, A. Grzechnik, K. Syassen, U. Schwarz, M. Hanfland, G. K. Rozenberg, P. Gorodetsky, and M. P. Pasternak, Phys. Rev. Lett. **87**, 125501 (2001).
[12] P. Mondal, D. Bhattacharya, and P. Choudhury, J. Phys.: Condens. Matter **18**, 6869 (2006); P. Mondal, D. Bhattacharya, P. Choudhury, and P. Mandal, Phys. Rev. B **76**, 172403 (2007).
[13] A. S. Korshunov, Yu. B. Kudasov, V. V. Platonov, and V. D. Selemir, *Book of Abstracts*, in Moscow International Symposium on Magnetism, Moscow, 20–25 June 2008, edited by N. Perov, V. Samsonova, and A. Semisalova (Moscow, 2008), p. 657.
[14] J.-S. Zhou and J. B. Goodenough, Phys. Rev. Lett. **96**, 247202 (2006).
[15] Y. Murakami, J. P. Hill, D. Gibbs, M. Blume, I. Koyama, M. Tanaka, H. Kawata, T. Arima, Y. Tokura, K. Hirota, and Y. Endoh, Phys. Rev. Lett. **81**, 582 (1998).
[16] M. v. Zimmermann, C. S. Nelson, Y.-J. Kim, J. P. Hill, D. Gibbs, H. Nakao, Y. Wakabayashi, Y. Murakami, Y. Tokura, Y. Tomioka, T. Arima, C.-C. Kao, D. Casa, C. Venkataraman, and Th. Gog, Phys. Rev. B **64**, 064411 (2001).
[17] J. Rodríguez-Carvajal, M. Hennion, F. Moussa, A. H. Moudden, L. Pinsard, and A. Revcolevschi, Phys. Rev. B **57**, R3189 (1998).
[18] F. Prado, R. Zysler, L. Morales, A. Caneiro, M. Tovar, and M. T. Causa, J. Magn. Magn. Mater. **196–197**, 481 (1999).
[19] Q. Huang, A. Santoro, J. W. Lynn, R. W. Erwin, J. A. Borchers, J. L. Peng, and R. L. Greene, Phys. Rev. B **55**, 14987 (1997).
[20] C. Ritter, M. R. Ibarra, J. M. De Teresa, P. A. Algarabel, C. Marquina, J. Blasco, J. Garcia, S. Oseroff, and S.-W. Cheong, Phys. Rev. B **56**, 8902 (1997).
[21] J. A. Alonso, M. J. Martínez-Lope, M. T. Casais, and M. T. Fernández-Díaz, Inorg. Chem. **39**, 917 (2000).
[22] P. Norby, I. G. K. Andersen, E. K. Andersen, and N. H. J. Andersen, J. Solid State Chem. **119**, 191 (1995).
[23] E. O. Ahlgren and F. W. Poulsen, Solid State Ionics **86–88**, 1173 (1996).
[24] J. J. U. Buch, T. K. Pathak, V. K. Lakhani, N. H. Vasoya, and K. B. Modi, J. Phys. D **40**, 5306 (2007).
[25] A. S. Moskvin, Physica B **252**, 186 (1998).
[26] A. S. Moskvin and I. L. Avvakumov, Physica B **322**, 371 (2002).
[27] A. S. Moskvin, Low Temp. Phys. **33**, 234 (2007).
[28] J. Töpfer and J. B. Goodenough, J. Solid State Chem. **130**, 117 (1997).
[29] A. Sartbaeva, S. A. Wells, M. F. Thorpe, E. S. Božin, and S. J. L. Billinge, Phys. Rev. Lett. **99**, 155503 (2007).
[30] G. Subías, J. Herrero-Martín, J. García, J. Blasco, C. Mazzoli, K. Hatada, S. Di Matteo, and C. R. Natoli, Phys. Rev. B **75**, 235101 (2007).
[31] A. M. Stoneham and M. J. L. Sangster, Philos. Mag. B **43**, 609 (1981).
[32] H. Katayama-Yoshida, K. Kusakabe, H. Kizaki, and A. Nakanishi, Appl. Phys. Express **1**, 081703 (2008).
[33] W. A. Harrison, Phys. Rev. B **74**, 245128 (2006).
[34] N. N. Kovaleva, A. V. Boris, C. Bernhard, A. Kulakov, A. Pimenov, A. M. Balbashov, G. Khaliullin, and B. Keimer, Phys. Rev. Lett. **93**, 147204 (2004).
[35] A. L. Shluger and A. M. Stoneham, J. Phys.: Condens. Matter **5**, 3049 (1993).
[36] N. N. Kovaleva, J. L. Gavartin, A. L. Shluger, A. V. Boris, and A. M. Stoneham, JETP **94**, 178 (2002).
[37] A. S. Moskvin, Phys. Rev. B **65**, 205113 (2002).
[38] J. Zaanen, G. A. Sawatzky, and J. W. Allen, Phys. Rev. Lett. **55**, 418 (1985).
[39] O. F. Schirmer, J. Phys.: Condens. Matter **18**, R667 (2006).
[40] T. M. Rice, in *Solid State Physics*, edited by H. Ehrenreich, F. Seitz, and D. Turnbull (Academic, New York, 1977), Vol. 32, p. 1.

[41] C. Zener, Phys. Rev. **82**, 403 (1951).
[42] M. Merz, N. Nucker, S. Schuppler, D. Arena, J. Dvorak, Y. U. Idzerda, S. N. Ustinovich, A. G. Soldatov, S. V. Shiryaev, and S. N. Barilo, Europhys. Lett. **72**, 275 (2005).
[43] C. Chaillout, A. Santoro, J. P. Remeika, A. S. Cooper, G. P. Espinosa, and M. Marezio, Solid State Commun. **65**, 1363 (1988).
[44] P. Huai and Keiichiro Nasu, J. Phys. Soc. Jpn. **71**, 1182 (2002).
[45] T. M. Rice and L. Sneddon, Phys. Rev. Lett. **47**, 689 (1981).
[46] A. S. Moskvin, N. S. Ovanesyan, and V. A. Trukhtanov, Hyperfine Interact. **1**, 265 (1975).
[47] G. J. Tomka, P. C. Riedi, Cz. Kapusta, G. Balakrishnan, D. McK. Paul, M. R. Lees, and J. Barratt, J. Appl. Phys. **83**, 7151 (1998).
[48] G. Allodi, M. Cestelli Guidi, R. De Renzi, and M. W. Pieper, J. Magn. Magn. Mater. **242–245**, 635 (2002).
[49] K. Shimizu, Y. Qin, and T. A. Tyson, Phys. Rev. B **73**, 174420 (2006).
[50] Cz. Kapusta and P. C. Riedi, J. Magn. Magn. Mater. **196–197**, 446 (1999).
[51] T. Inami, T. Fukuda, J. Mizuki, S. Ishihara, H. Kondo, H. Nakao, T. Matsumura, K. Hirota, Y. Murakami, S. Maekawa, and Y. Endoh, Phys. Rev. B **67**, 045108 (2003).
[52] I. L. Avvakumov and A. S. Moskvin (unpublished).
[53] A. S. Moskvin, I. G. Bostrem, and A. S. Ovchinnikov, JETP Lett. **78**, 772 (2003); A. S. Moskvin, Phys. Rev. B **69**, 214505 (2004).
[54] A. M. Kadomtseva, A. S. Moskvin, I. G. Bostrem, B. M. Wanklyn, and N. A. Khafizova, Zh. Eksp. Teor. Fiz. **72**, 2286 (1977).
[55] R. Micnas, J. Ranninger, and S. Robaszkiewicz, Rev. Mod. Phys. **62**, 113 (1990).
[56] K. Tobe, T. Kimura, Y. Okimoto, and Y. Tokura, Phys. Rev. B **64**, 184421 (2001).
[57] M. W. Kim, S. J. Moon, J. H. Jung, J. Yu, S. Parashar, P. Murugavel, J. H. Lee, and T. W. Noh, Phys. Rev. Lett. **96**, 247205 (2006).
[58] N. N. Loshkareva, Yu. P. Sukhorukov, E. V. Mostovshchikova, L. V. Nomerovannaya, A. A. Makhnev, S. V. Naumov, E. A. Gan'shina, I. K. Rodin, A. S. Moskvin, and A. M. Balbashov, JETP **94**, 350 (2002).
[59] A. S. Moskvin, E. V. Zenkov, Yu. D. Panov, N. N. Loshkareva, Yu. P. Sukhorukov, and E. V. Mostovshchikova, Phys. Solid State **44**, 1519 (2002).
[60] Yu. P. Sukhorukov, N. N. Loshkareva, E. A. Gan'shina, E. V. Mostovshchikova, I. K. Rodin, A. R. Kaul, O. Yu. Gorbenko, A. A. Bosak, A. S. Moskvin, and E. V. Zenkov, JETP **96**, 257 (2003).
[61] E. V. Mostovshchikova, N. G. Bebenin, and N. N. Loshkareva, Phys. Rev. B **70**, 012406 (2004).
[62] N. N. Loshkareva, Yu. P. Sukhorukov, E. A. Neifel'd, V. E. Arkhipov, A. V. Korolev, V. S. Gaviko, E. V. Panfilova, V. P. Dyakina, Ya. M. Mukovskii, and D. A. Shulyatev, JETP **90**, 389 (2000).
[63] Y. Okimoto, T. Katsufuji, T. Ishikawa, A. Urushibara, T. Arima, and Y. Tokura, Phys. Rev. Lett. **75**, 109 (1995); Y. Okimoto, T. Katsufuji, T. Ishikawa, T. Arima, and Y. Tokura, Phys. Rev. B **55**, 4206 (1997).
[64] J. H. Jung, K. H. Kim, T. W. Noh, E. J. Choi, and Yu. Jaejun, Phys. Rev. B **57**, R11043 (1998).
[65] T. Chatterji, F. Fauth, B. Ouladdiaf, P. Mandal, and B. Ghosh, Phys. Rev. B **68**, 052406 (2003).
[66] M. C. Sánchez, G. Subías, J. García, and J. Blasco, Phys. Rev. Lett. **90**, 045503 (2003).
[67] X. Qiu, Th. Proffen, J. F. Mitchell, and S. J. L. Billinge, Phys. Rev. Lett. **94**, 177203 (2005).
[68] V. B. Podobedov, A. Weber, D. B. Romero, J. P. Rice, and H. D. Drew, Phys. Rev. B **58**, 43 (1998).
[69] M. N. Iliev, M. V. Abrashev, H. G. Lee, V. N. Popov, Y. Y. Sun, C. Thomsen, R. L. Meng, and C. W. Chu, Phys. Rev. B **57**, 2872 (1998).
[70] R. Kruger, B. Schulz, S. Naler, R. Rauer, D. Budelmann, J. Backstrom, K. H. Kim, S.-W. Cheong, V. Perebeinos, and M. Rubhausen, Phys. Rev. Lett. **92**, 097203 (2004).
[71] N. N. Loshkareva, Yu. P. Sukhorukov, E. A. Gan'shina, E. V. Mostovshchikova, R. Yu. Kumaritova, A. S. Moskvin, Yu. D. Panov, O. Yu. Gorbenko, and A. R. Kaul, JETP **92**, 462 (2001).
[72] M. T. Causa, G. Alejandro, R. Zysler, F. Prado, A. Caneiro, and M. Tovar, J. Magn. Magn. Mater. **196–197**, 506 (1999).
[73] M. Tovar, G. Alejandro, A. Butera, A. Caneiro, M. T. Causa, F. Prado, and R. D. Sanchez, Phys. Rev. B **60**, 10199 (1999).
[74] I. Solovyev, N. Hamada, and K. Terakura, Phys. Rev. Lett. **76**, 4825 (1996).
[75] A. V. Korolyov, V. Ye. Arkhipov, V. S. Gaviko, Ya. Mukovskii, A. A. Arsenov, T. P. Lapina, S. D. Bader, J. S. Jiang, and V. I. Nizhankovskii, J. Magn. Magn. Mater. **213**, 63 (2000).
[76] M. Paraskevopoulos, F. Mayr, J. Hemberger, A. Loidl, R. Heishele, D. Maurer, V. Müller, A. A. Mukhin, and A. M. Balbashov, J. Phys.: Condens. Matter **12**, 3993 (2000).
[77] P. A. Algarabel, J. M. De Teresa, J. Blasco, M. R. Ibarra, C. Kapusta, M. Sikora, D. Zajac, P. C. Riedi, and C. Ritter, Phys. Rev. B **67**, 134402 (2003).
[78] J. A. Souza, J. J. Neumeier, R. K. Bollinger, B. McGuire, C. A. M. dos Santos, and H. Terashita, Phys. Rev. B **76**, 024407 (2007).
[79] I. M. Fita, R. Szymczak, M. Baran, V. Markovich, R. Puzniak, A. Wisniewski, S. V. Shiryaev, V. N. Varyukhin, and H. Szymczak, Phys. Rev. B **68**, 014436 (2003); V. Markovich, I. Fita, A. I. Shames, R. Puznyak, E. Rozenberg, Ya. Yuzhelevski, D. Mogilyansky, A. Wisniewski, Ya. M. Mukovskii, and G. Gorodetsky, J. Phys.: Condens. Matter **15**, 3985 (2003).
[80] S. B. Oseroff, M. Torikachvili, J. Singley, S. Ali, S.-W. Cheong, and S. Schultz, Phys. Rev. B **53**, 6521 (1996).
[81] G. Allodi, R. De Renzi, G. Guidi, F. Licci, and M. W. Pieper, Phys. Rev. B **56**, 6036 (1997).
[82] F. Bolzoni and R. Cabassi, J. Appl. Phys. **103**, 063905 (2008).
[83] J.-H. Park, C. T. Chen, S.-W. Cheong, W. Bao, G. Meigs, V. Chakarian, and Y. U. Idzerda, Phys. Rev. Lett. **76**, 4215 (1996).
[84] G. Subias, J. Garcia, M. G. Proietti, and J. Blasco, Phys. Rev. B **56**, 8183 (1997).
[85] T. A. Tyson, Q. Qian, C. C. Kao, J. P. Rueff, F. M. F. de Groot, M. Croft, S. W. Cheong, M. Greenblatt, and M. A. Subramanian, Phys. Rev. B **60**, 4665 (1999).
[86] B. Gilbert, B. H. Frazer, A. Belz, P. G. Conrad, K. H. Nealson, D. Haskel, J. C. Lang, G. Srajer, and G. De Stasio, J. Phys. Chem. A **107**, 2839 (2003).
[87] J. Jiménez-Mier, D. L. Ederer, and T. Schuler, Phys. Rev. B **70**, 035216 (2004).
[88] M. Croft, D. Sills, M. Greenblatt, C. Lee, S.-W. Cheong, K. V. Ramanujachary, and D. Tran, Phys. Rev. B **55**, 8726 (1997); R. S. Liu, J. B. Wu, C. Y. Chang, J. G. Lin, C. Y. Huang, J. M. Chen, and R. G. Liu, J. Solid State Chem. **125**, 112 (1996).

[89] H. L. Ju, H.-C. Sohn, and K. M. Krishnan, Phys. Rev. Lett. **79**, 3230 (1997).
[90] V. R. Galakhov, M. Demeter, S. Bartkowski, M. Neumann, N. A. Ovechkina, E. Z. Kurmaev, N. I. Lobachevskaya, Ya. M. Mukowskii, J. Mitchell, and D. L. Ederer, Phys. Rev. B **65**, 113102 (2002).
[91] G.-L. Liu, J.-S. Zhou, and J. B. Goodenough, Phys. Rev. B **70**, 224421 (2004).
[92] Yong-Jihn Kim, Mod. Phys. Lett. B **12**, 507 (1998).
[93] M. Kasai, T. Ohno, Y. Kanke, Y. Kozono, M. Hanozono, and Y. Sugita, Jpn. J. Appl. Phys., Part 2 **29**, L2219 (1990); M. Kasai, Y. Kanke, Y. Ohno, and Y. Kozono, J. Appl. Phys. **72**, 5344 (1992).
[94] A. V. Mitin, G. M. Kuzmicheva, and S. I. Novikova, Zh. Neorg. Khim. **42**, 1953 (1997).